Sudan University of Science & Technology
College of Postgraduate Studies

Synthesize, Characterize, and Properties Study of the Polystyrene (Cork) doped by Aluminum Oxide (Al_2O_3)

تولیف ووصف ودراسة خصائص البولیسترین (الفلین) المشوب بأكسيد الألومنيوم (Al2O3)

A thesis submitted for the requirements of the PhD of Science in Physics

Prepared by

Tamador Almardi Albashir Abdelrahim

Supervisor
Dr. Mahmoud Hamid Mahmoud Hilo

Jan - 2021

الإستهلال

بسم الله الرحمن الرحيم

8 7

Æ Å Ä Â Á À M

L Î Í Ì Ë Ê É È Ç

سورةالإسراء: الآية ٨٥

Acknowledgement

Thanks to God before and after.

I wish to thank everyone who contributed with me or helped me from near or far during the period of completing this work.

Dedication

I dedicate this research to:

My Father

My Mother

My brothers and sisters

My colleagues and professors

Abstract

Cork is considered one of the polymers of very low industrial value and is used only for secondary purposes such as packaging, and it is possible to have any other uses of high value by doping the cork with materials that can improve its physical properties, this research aimed to synthesize and characterize the optical, and structural properties of pure Polystyrene (200 grams) Cork, and Polystyrene (200 grams) Cork doped by Aluminum oxide in ratios (0.1 to 0.9) M. To prepare Aluminum oxide , aluminum nitrate (AL (NO3)39H2O)) was used (as a source of Aluminum hydroxide, provided by (LOBA CHEMIE) company, with a molecular weight of 375.13 and a concentration of 98%, which is a white powder that is soluble in water, it was prepared at a temperature of (80) degrees Celsius for each Samples with different concentrations ranging from (0.1, 0.2, 0.3, 0.4, 0.5, 0.6, 0.7, 0.8, 0.9) M, by adding N, N-Dimethylformamide for HPLC as an simulating agent and precipitant, and then by Sol-Gel method at a temperature of 80°C for 60 minutes, samples of doped cork were deposited on glass slides. By using the ultraviolet technique (UV-VIS), the Absorbance spectra were recorded within the wavelength range of (200-800) nm. The results showed that the absorbance decreased with increasing the cork doping percentage. The basic absorption peaks of the cork tends towards the low photon energy (red shift) when increasing the doping rates of Aluminum oxide, while it was tending towards the high energy (blue shift) photon at the cork before doping, and that is through the absorption coefficient values that were calculated from the absorbance spectrum, which is greater than Likewise, the optical parameters of reflectivity, extinction coefficient, and refractive index were calculated. The energy gap of the cork doped by Aluminum oxide is small compared to the energy gap of the pure polystyrene cork. It has been concluded that the Aluminum oxide ratios with different molar

values confirm the cause of the energy gap shifts, and through X-ray diffraction, where the results showed that all the prepared samples are multi-crystallized of the types (cubic, mono, triple and hexagonal). And it was found that the preferred direction of growth is the level (2 1 1), and the crystal size of all the prepared samples was calculated, and it was found that it increases with the increase of doping percentage. Also, the density and number of crystals were calculated as each of them decreases with the increase of the doping percentage.

المستخلص

يعتبر الفلين من البوليمرات ذات القيمة الصناعية المنخفضة للغاية ويستخدم فقط لأغراض ثانوية مثل التعبئة والتغليف، ومن الممكن أن يكون له أي استخدامات أخرى ذات قيمة عالية عن طريق تشويب الفلين بمواد يمكنها تحسين خصائصه الفيزيائية ، وهذا البحث يهدف إلى توليف وتوصيف الخصائص البصرية والتركيبية للبوليسترين النقي (200 جرام) -الفلين- والبوليسترين (200 جرام) الفلين المشوب بأكسيد الألومنيوم بنسب (0.1 إلى 0.9) %. لتحضير أكسيد الألومنيوم تم استخدام نترات الألومنيوم (AL (NO3) 39H2O) (المقدم من شركة (LOBA CHEMIE) بوزن جزيئي 375.13 وبتركيز 98٪ وهو مسحوق أبيض قابل للذوبان في الماء وتم تحضيره. عند درجة حرارة (80) درجة مئوية لكل عينة بتركيزات مختلفة تتراوح من (0.1 ، 0.2 ، 0.3 ، 0.4 ، 0.5 ، 0.6 ، 0.7 ، 0.8 ، 0.9) %) كمصدر لهيدروكسيد الألومنيوم، وذلك عن طريق إضافة N - N- ثنائي ميثيل فورماميد لـ HPLC كعامل محفز. ثم باستخدام طريقة Sol-Gel عند درجة حرارة 80 درجة مئوية لمدة 60 دقيقة ، تم طلاء عينات من الفلين المحضر على شرائح زجاجية. ثم باستخدام تقنية الأشعة فوق البنفسجية (UV-VIS) ، تم تسجيل أطياف الامتصاصية ضمن مدى الطول الموجي (200-800) نانومتر. أظهرت النتائج أن الامتصاصية تزيد مع زيادة نسبة تشويب الفلين. تميل قمم الامتصاص الأساسية للفلين نحو طاقة الفوتون المنخفضة (الانزياح الأحمر) عند زيادة معدلات التشويب بأكسيد الألومنيوم ، بينما كان يميل نحو الفوتون عالي الطاقة (الانزياح الأزرق) في الفلين قبل التشويب بأكسيد الألومنيوم، وذلك من خلال قيم معامل الا متصاص التي تم حسابها من طيف الامتصاصية. وبالمثل تم حساب الخصائص الضوئية للانعكاسية ومعامل الخمود ومعامل الانكسار. فجوة الطاقة في الفلين المشوب بأكسيد الألومنيوم صغيرة مقارنة بفجوة الطاقة لفلين البوليسترين النقي. وقد تم الاستنتاج أن نسب أكسيد الألومنيوم بقيم مولارية مختلفة تؤكد سبب انزياحات فجوة الطاقة ، ومن خلال حيود الأشعة السينية ، حيث أظهرت النتائج أن جميع العينات المحضرة متعددة التبلور من الأنواع (مكعب ، أحادي ، ثلاثي وسداسي). ووجد أن الاتجاه المفضل للنمو هو المستوى (2 1 1) ، وقد تم حساب الحجم البلوري لجميع العينات المحضرة ، ووجد أنه يزداد مع زيادة نسبة التشويب. كما تم حساب كثافة وعدد البلورات حيث يتناقص كل منها مع زيادة نسبة التشويب.

Table of contents

List of tables

List of figures

Chapter One
Introduction

1. Introduction

Cork is one of the oldest substances known to mankind, a material that is based like a sponge and its origin is plant and is lightweight, and a insulating material also worse against water, sound, heat and electricity, it does not absorb water easily, and it is also characteristic of cork that it bears high pressure, and this substance appeared in the centuries BC where the barges were made of them, as well as to float fishing nets being a light material floating on the sea surface, and then used as pipe plugs [1]. It does not absorb water easily and can be compressed considerably, but returns to its first state after the pressure has subsided. Since the 4th century B.C., people have used corks and the Romans have worn cork sandals, and they have used cork to float shipyards and fishing nets [2, 3]. Cork plugs have been made since the 17th century. The cork is produced after obtaining the outer shell of the cork tree as it contains an outer layer of coarse sand which is brown, and is adjacent to the cork material and attached to the so-called tannic acid, the first step begins with the skimming of the outer layer, and the crust is placed in boiling water until the material becomes soft and the acid separates from it, after which it is easy to form a whole slab of cork, and the cork differs in quality and density and then is shipped to be used in industry [4, 5]. The cork tree has a remarkable capacity to create suberose tissue from its inner bark. This tissue, formed specifically by the phylogeny of the cork oak (the tissue responsible for the formation of new cells), derives its name from the Latin super (5cork). The life cycle of the Cork oak produces three qualities of supersize tissue virgin cork, reproduction cork from the second strip-ping; and reproduction cork from subsequent strips [6]. The

thickest supersize layer is generally formed in the growing cycle following cork extraction, after which the cork produced per year diminishes progressively until the next extraction [7-9]. Cork (or cork, the botanical designation of this vegetable tissue) is a protective layer of supersized dead cells, formed from phylogeny tissue. The phylogeny has meristematic (cell generation) capacity. After cellular division, the new cells do not have their final dimensions and subsequently undergo growth in the protoplasm (cellular interior); in this way Cork tissue continues to thicken and the tree perimeter increases. Tissue growth ceases in winter and starts again at the beginning of the spring. The Cork period is April-October; the winter standstill is manifested in highly visible dark zones, marking off the cork produced each year. The annual addition of Cork layers corresponding to lenticular evolution, determines the definition of lenticular channels (radial and oriented pores) where the oxygenation of meristematic tissue takes place [10, 11]. The main function of meristematic tissues mitosis (cellular division); these cells are small, thin-walled and with no specialized features. Cork acts as a barrier between the atmosphere and the cortex of the stem, and lenticels serve as mass transfer channels for water and gases. The phylogenic tissue of cork oak is active throughout the tree's life [12].

1.2 Problem of the study

Some polymers have conductive properties which enable them to flow the electricity, but the large number of polymers are classified to be insulators and both states make polymers not in the right state to be used in industrial field, especially as semiconductors or in the application of solar energy. Doping of polymers with metallic oxides may allow them to achieve semiconducting properties that can open the door widely to be used in the field of electronics, radiation filters, multijunctions, and solar applications.

One of the most important things that lead to this research is that the material of the polystyrene (Cork) is available and cheap that can be a good choice if its properties match the semiconducting range.

1.3 Aim of the study

The general objectives of this study is to synthesize and Characterize the Polystyrene (Cork) doped by Aluminium Oxide (Al_2O_3) to improve its optical and structural properties using the UV-VIS, XRD, FTIR techniques, and the specific aims of the research is to prepare the aluminum oxide, prepare the cork solutions and doped them by aluminum oxide in different rate of molars, deposit the samples on the glass slights, and finally characterizing the samples by all the techniques used in the research.

1.4 The significance of the Study

Cork is considered one of the polymers of very low industrial value and is used only for secondary purposes such as packaging, and it is possible to have any other uses of high value by doping the cork with materials that can change its physical properties, so the significance of this study comes from the ability of finding a new way to benefit highly from the doping of the Cork and its abundance in both type natural and manufactured Cork.

1.5 Method

This research will follow the applied or experimental method to synthesize and characterize the polystyrene (Cork) doped with aluminum oxide so as to prepare the sample in slight of glass.

Ten samples will be prepared by changing the doping amount at the aluminum oxide from (0.1 to 0.9) percent and the sol-gel method will be used. Also characterization of the samples by techniques such as XRD, UV, and FTIR will be applied on to the samples and a wide discussion will be done the scope.

This study will come in four chapters ,chapter one for introduction ,chapter two will include the theoretical background and literature review , chapter three states the experimental and result of the study, finally chapter four will be for discussion, conclusion and recommendations .

1.6 Previous studies

1. researchers, **Natalia Ferreira Braga, at el,** (2020), studied the **Effect of Carbon Nano tubes (CNT) Functionalization and Maleic Anhydride-Grafted Poly (trimethyleneterephthalate) (PTT-g-MA) on the Preparation of Antistatic Packages of PTT/CNT Nano composites** and they concluded that, The effect of chemical Functionalization of carbon nano tubes and the addition of a compatibilizer agent (PTT-g-MA) on thermal, mechanical, electrical, and morphological properties of PTT/CNT nano composites were evaluated. Stability dispersion in water showed that Functionalization improved the dispersion of CNT due to an increase in the number of polar interactions performed by the functional groups. Also, Raman spectroscopy revealed defects in the CNT structure due to its Functionalization. Moreover, FTIR showed the appearance of two new bands related to creation of functional groups inserted on CNT surface after Functionalization. DSC analysis showed that the CNT or

CNT f did not act as a nucleation agent but generated a confinement effect of the polymeric chains since no significant increase in PTT crystalline degree was observed after the insertion of CNT or CNT f [13]

2. Researchers, Subramanian Senthilkumar, and Annamalai Rajendran, (2017), studied the **Synthesis, characterization and electrical properties of nano metal and metal-oxide doped with conducting polymer composites by in-situ chemical polymerization** and they concluded that pure polyaniline, n-Al2O3 Pani and n-Al Pani were synthesized by adopting a facile chemical oxidation polymerization method. The structure of the pure pani and its composites has been confirmed by FT-IR study. The average crystalline sizes have been estimated to be around n-Al pani and n-Al2O3 pani is 31 and 38nm. The FESEM morphology showed that the Pani and n-Al pani and n-Al2O3 pani has the morphological modification due to doping and EDX study reveals that the aluminum and aluminum oxide nano composites is evenly distributed through the polymer matrix. The increased conductivity was attributed to the formation of a better charge transport network in the relatively insulating PANI matrix. The improvement in the electrical conductivities of these composites is expected to enhance the potential application of the polymer. The results show enhancement in photo degradation of dyes is due to Al polyaniline crystallite size increase and decrease in particle size, which leads to higher surface and adsorptive nature.

3. Researchers, **Yasser Zare and KyongYop Rhee, (2019)**, studied the **Electrical Conductivity of Polymer Nanocomposites Assuming the Interphase Layer Surrounding Carbon Nanotubes** and they concluded that the effective volume fraction of CNT, percentages of percolated filler after percolation threshold and electrical conductivity in PCNT were expressed assuming the tunneling effect by interphase layer around

nanoparticles. Thin and long CNT, thick interphase, and low waviness caused positive effects on the fraction of percolated CNT, but a high effective filler fraction was only obtained by thin CNT and thick interphase. Thin and long CNT caused a low distance among nanotubes in PCNT, which increased the probability of connection and networking. Also, a thick interphase showed a strong contribution to the connection of CNT, because it can push the separated nanotubes to form a conductive network. The waviness also decreased the effective length of nanotubes, which weakened their percolation and joining. According to these explanations, it was logical to obtain the highest conductivity of PCNT by the thinnest and the longest CNT, the thickest interphase, and the smallest waviness. These parameters effectively changed the effective properties of CNT and network; so, they significantly governed the electrical conductivity of PCNT. It was also reported that a low value of " φ e f f " did not change the conductivity of PCNT, but the smallest φ p = 0.001 and the highest φ e f f = 0.06 produced the highest conductivity of 2500 S/m by conventional model. Also, the highest conductivity of 7000 S/m was observed at the highest values of fiu = 0.5 and φ e f f = 0.06 based on the developed model. These evidences demonstrated that the low value of " φ p " as well as the great ranges of both "fiu" and " φ e f f " terms induced the high conductivity of PCNT.

4. Researchers**,** PATRICIA NORDELL, (2011), studied the ALUMINIUM OXIDE – POLYETHYLENE-CO-BUTYL ACRYLATE) NANOCOMPOSITES: SYNTHESIS, STRUCTURE, TRANSPORT PROPERTIES AND LONG-TERM PERFORMANCE and they concluded the Surface modification by silanization rendered partially silane-covered nanoparticles of both particle types, Nanodur (ND) and Nanoamor (NA) and for both types of silane (octyltriethoxy and aminopropyltriethoxysilane). The amount of silane grafted to the NA

particle surfaces was higher, since these particles had approximately five times more hydroxyl groups per surface area. The particle shape and amount of hydroxyl groups on the particle surfaces had a major influence on the final material structure: the dispersion of the ND particles was satisfactory, whereas all NA composites exhibited a many m-sized agglomerates. Especially the octyl-coated ND particles were well-distributed in EBA-13. It is believed that the higher amount of hydroxyl groups on the NA particle surfaces, and the flatter geometry of these particles resulted in denser agglomerates, during the post-drying step after the surface treatment. The materials based on EBA-28, showed inhomogeneous dispersion levels. This was most probably due to the lower melt viscosity of this polymer compared to EBA-13, resulting in insufficient shear forces during compounding.

Chapter two

Theoretical Background and Literature Review

2.1 Introduction

This chapter tackles a general description in the theoretical part which describes the properties that has been studded in the research and the physicalconcepts, and gives some mathematical relations that used to calculate and discuss the results.

2.2 Cork (Polystyrene)

Cork is a material extracted from the bark of newborns, and it is a material, light in weight, which is good, and it is able to update to its natural state after the pressure is removed. People have used cork since the fourth century BC. M. The Romans wore cork sandals, and we used cork to float marinas and fishing nets. Cork stoppers have been in use since the 17th century AD Cork Uses Most cork is used as an insulating material. For this purpose it is collected and compressed in the form of sheets and tube caps. In this way, cork covers the walls and freezer tubes of thousands of refrigerated storage plants, meat preservation plants, ice cream factories, and oil refineries. Cork floats in the water, hence it is used in the manufacture of rafts and fishing net buoys. Floor liners are made by mixing cork powder with linseed oil, and this paste is spread over hemp or burlap. Floors, walls and ceilings can be made soundproof using cork panels. One of the primary uses of cork is its use in bottle stoppers, where thin gaskets of cork are used to seal the inner portion of the flask's metal caps. In addition, cork is used in waterproofing covers, in balloon fabric, and as filler for spray guns. Cork mulch is burned to make Spanish black, or cork black, a dye used by artists.

It is a natural resin; synthetics are not used in the manufacture of cork materials. According to its molecular structure, it resembles fats. It is characterized by high resistance to oxygen, as well as mineral acids and

bacteria. In addition, thanks to this component, the shell tissues are elastic and have a low level of thermal conductivity. This substance is a complex mixture of aromatic polymers. Together with the fibers (cellulose), they are responsible for the strength of the cork.

There are approximately 40 million cells in every cubic centimeter of this material. The shape of each is a polyhedron consisting of 14 faces, in which the inner space is filled with an oxygen-nitrogen gaseous mixture that does not contain a mixture of carbon dioxide. All cells are separated from one another by the intercellular septum. Thanks to this peculiar structure, cork products have remarkable thermal insulation properties, do not let moisture and gaseous substances pass through them. Cork is a natural, renewable, sustainable raw material that has been used for many centuries. As a result of this very long term interest, the scientific literature on cork is extensive. The present review focuses on the chemical composition, physical and mechanical properties of cork and on its products and sub-products. The substantial efforts to fully characterize cork, as well as new developments and evolving research, are reviewed, beginning with its histology, growth and morphology (at macro- and microscales). The chemical structure is analyzed in detail, covering both the materials that form the wall structure and the low molecular weight, extractable components. The unique properties of cork are discussed and correlated with current knowledge on morphology and chemical structure. Finally, the important industrial applications of cork are reviewed, in the context of research to provide cork with novel, high added-value applications.Cork is the bark of the oak (Quercussuber L.) which isperiodically harvested from the tree, usually every 9–12years, depending on the culture region is the botanical name for a slow growing, evergreen oakthat flourishes only in specific regions of the WesternMediterranean (Portugal, Spain, Southern France, partof Italy,

North Africa) and China [14-19].This tree requires a great deal of sunlight and a highly unusual combinationof low rainfall and somewhat high humidity. Europe hasabout 60% of the total production area (cork forests)and produces more than 80% of the world's cork [15].Portugal is the major cork producer and processes aboutthree-quarters of all the cork. The quality and thicknessof the bark vary according to a tree's specific growth conditions [16-19].

2.2.1 Morphology

The cork tree has a remarkable capacity to create suberose tissue from its inner bark. This tissue, formed specifically by the phylogeny of the cork oak (the tissue responsible for the formation of new cells), derives itsname from the Latin super (5cork). The life cycle of the Cork oak produces three qualities of suberize tissuevirgin cork, reproduction cork from the second strip-ping; and reproduction cork from subsequent strips [15]. The thickest supersize layer is generally formed in thegrowing cycle following cork extraction, after which thecork produced per year diminishes progressively until the next extraction [13, 17].

2.2.2 Final remarks

Cork has a remarkable combination of mechanical, chemical and morphological characteristics. This natural organic material continues to be widely used. It has evolved from simple, direct usage of the raw material, through products involving some industrial transformation to the point where it now represents a potential source material for high technology industries (pharmaceutical, ceramic, etc.).This evolution has been supported and facilitated by the use of increasingly complex characterization techniques that set the foundations for a realization of the full potential of cork. From the initial microscopic observations of Hooke, cork has been the subject of diverse mechanical, physical, chemical and morphological characterization, lately including thermally stimulated

discharge current analysis, nuclear magnetic resonance and gas chromatography–mass spectroscopy.

Cork is resilient, strong (high specific strength), impervious to water, has a near zero Poisson coefficient, very low thermal conductivity, low density and a complex chemical structure. This combination of properties provides cork with characteristics hard to match with other materials: excellent sealing ability and ease of removal, thermal comfort and damping for walking, thermal insulation at very low temperatures, among others.

Cork has proved to be a highly adaptable material, giving rise to products of low and high incorporated technology. The continuing interest, the increasing glydetailed characterization and society's growing requirements for natural, renewable and sustainable raw materials will create novel market areas. In the research field, chemical characterization and some physical properties still pose challenges and a significant contribution can be anticipated in areas of concern to the development of novel applications for cork and cork incorporating products.

2.3 Optical Properties

The study of the optical properties of materials is of great importance because it gives a lot of Information about the type of electronic transitions that occur in the material, in addition to leaving the energy beams; it also describes the properties that determine the interaction of light with matter.

When the energy of the radiation absorbed by the semiconductor is greater or equal, it is approximately to a value the energy gap (Eg), as it causes an electron to move from the valence beam filled with electrons to The conduction beam is devoid of electrons, so the area of the spectrum of the incident rays is defined and where it starts P are electrons moving at the absorption edge, and the amount differs in the energy between the

lowest point in the conduction beam and the energy of the highest point in the valence beam is called the optical energy gap [18].

2.3.1 Optical Transmittance

Optical transmittance (T) is the ratio between the intensity of the radiation transmitted from the thin membrane (I_T) to the intensity of the fallen radiation (I_0) and expressed by the relation [7].

$$T = \frac{I_T}{I_0} \qquad (1)$$

The semi-conductor material when exposed to a beam of radiation, part of the falling rays will be carried out and the transmittance of the rays depends on the fallen photons and the properties of the semiconductor material, as well as the thickness of the membranes and the temperature of the preparation and the percentage of addition of impurities

2.3.2 Optical Absorbance

Optical absorption (A) is the ratio between the intensity of radiation absorbed by the membrane (I_A) to the intensity of the radiation falling on it (I_0), is known as absorption, as it represents the decrease in the energy of electromagnetic radiation when entering the membrane, it depends on the nature and the thickness of the semiconductor and expressed by the relation [20].

$$A = \frac{I_A}{I_0} \qquad (2)$$

2.3.3 Optical reflexivity

The optical reflectance (R) the ratio between the intensity of the radiation falling, to the intensity of the radiation reflected at the limit between the two mediums, it is known as reflectivity. Reflexivity can be calculated according to the law of energy conservation and by knowing the value of both transmittance (T) and absorption (A) [20].

$$R + T + A = 1 \qquad (3)$$

2.3.4 Absorption Coefficient

Absorption coefficient is the ratio of the decrease in the flux of radiation energy falling relative to the unit of distance towards the spread of the wave within the medium known as absorption coefficient, it depends on the properties of the semiconductor in terms of the energy gap and the type of electronic transmissions that occur between the energy band and the energy of the fallen photons through the relation [21-23]

$$E = h\upsilon \qquad (4)$$

And finally we find that the absorption coefficient can be written in terms of the absorbance (A) by the following equation

$$\alpha = 2.303\frac{A}{t} \qquad (5)$$

Where t denote the thickness of the layer

2.3.5 Refractive Index

Refractive index is the ratio between the speed of light in the vacuum (c) to its speed in the medium (v) which is called the refractive coefficient (n), and the refractive index depends on the type of material and its crystal structure and is expressed by the following equation [24].

$$n = \left[\left(\frac{1+R}{1-R}\right)^2 - \left(k_0^2 + 1\right)\right]^{\frac{1}{2}} + \frac{1+R}{1-R} \qquad (6)$$

2.3.6 Extinction Coefficient

The extinction coefficient is the amount of energy absorbed in the thin membrane, and the energy absorbed by the material from the fallen photons, in other words, it represents the extinction or attenuation occurring in the electromagnetic wave inside the material [25].

$$K_0 = \frac{\alpha\lambda}{4\pi} \qquad (7)$$

2.3.7 Optical Energy Gap

Energy gap is an important visual constant, and is a function of temperature as its value changes slightly with the change of temperature where the energy gap increases in some semiconductors while in others, the energy gap for pure semiconductor is not completely empty where there are local levels resulting from synthetic defects. The energy gap for the direct electronic transmissions allowed can be calculated by plotting the relation between $(h\upsilon)$ and $(\alpha\upsilon h)^2$ by extending the best straight line that is a definite extension of the photon energy axis. The value of the energy gap is determined by the intersection point with the x axis at which $(\alpha\upsilon h)^2 = o$ [26].

2.4 Structural Properties

The structural properties are an important method for studying the crystal structure of layers, and this is done through the use of X-ray diffraction, and FTIR. First the X-ray diffraction analysis is used to know the nature of the crystal structure and the main crystalline phases, and that is to know the oriented direction of the prepared layers under certain conditions, as the general principle of diffraction depends on the phenomenon of interference that occurs when the movement of a wave is dispersed at a number of centers of atoms and as a result, either interference occurs Constructive or destructive interference.

The English scientist (Bragg) assumed a simple pattern of the crystal structure, by means of which he could know the direction of the X-ray diffraction from the crystal after its fall in practice, and this model states that the different levels that are composed of the crystal atoms can reflect the X-rays [19, 20].

$$n\lambda = 2d\sin\theta \qquad (8)$$

Where (d): the distance between two successive atomic levels and (Ɵ) the diffraction angle

(n) Integer (1, 2, 3…), and λ: the X-ray wavelength

As the reflection of Braque occurs only when the wavelength of the incident X-rays through which it is possible to obtain a reflection from a plane that has coordinates smaller or equal to twice the interface distance between two successive crystals, as shown in the figure below, therefore, visible light cannot be used to study the crystal structure, that is, the Braque condition For reflection is $\lambda \leq 2d_{hkl}$

Lattice constants: Knowing the compositional factors of a substance that depends on the X-ray diffraction spectrum is important in explaining many of the physical properties of the material. Thus the lattice constant (a) can be calculated using the following equation

$$d_{hkl} = \frac{a}{\left(h^2 + k^2 + l^2\right)^{\frac{1}{2}}} \qquad (9)$$

Average particle size: The average grain size is calculated using the (Scherer's Formula)

$$D_{av} = \frac{k\lambda}{\beta \cos\theta} \qquad (10)$$

Since k: the forming factor equals 0.94

λ : The wavelength of the X-ray used

θ: Bragg diffraction angle

β : Full width at half-maximum in (r ad) (FWHM)

Second, the FTIR The idea of a device the goal of an FT-IR absorption spectrometer is to absorb shock and light at every wavelength. The most intense way to do this, dispersion spectroscopy is to illuminate a sample, measure the amount of light, and the frequency of each wave is different. (For example this is how UV rays work).

Fourier spectroscopy (FT-IR) is the method for obtaining information from shining a monochromatic light beam (a mid-beam of only one wavelength) this technique scans a beam that contains many frequencies of light simultaneously and measures the amount of absorption that the beam absorbs from the sample.

The beam is modified to have a different set of frequencies, which gives a second data point.

This process is repeated many times. The computer takes all this data and works backwards to deduce what absorption is at each wavelength. The beam described above is created by starting with a broadband light source - one containing the full spectrum of the wavelengths to be measured. The lamp is illuminated in the Michelson interferometer, a specific configuration of mirrors, one of which is driven by a motor. As this mirror moves, To the desired result (light absorption per wavelength). It turns out that the required processing is a popular algorithm called the Fourier transform (hence the name "Fourier transform spectroscopy"). The raw data is sometimes called "interference"[27].

Features of FT-IR High analysis speed the advantage of velocity was realized because all the wavelengths in the spectral field were examined together and the absorption spectra were displayed in real time.

Lack of cracks and mesh barriers the absence of a minimum elemental energy makes it possible to have the entire energy of the resulting beam at any point in time. On the other hand, due to the high scanning speed of several spectra added together and the average results of the signal in several fields, it improved their sensitivity. Simultaneous frequency modulation although the Nicholson interferometer regulates all of the existing frequencies simultaneously, there is nothing equal to stray light that helps clarify the spectrum.

Built-in wavelength calibration the device is based on the He-Ne laser, which is used internally for self-calibration of individual frequencies to have an accuracy of more than (0.01) cm-1. However it is still advisable to run the reference spectrum of the thin polystyrene layer occasionally and compare it to the standard spectrum kept in the reference library at the time of fixation.

Spectral interference feature Spectral interference feature that helps to compare with standard reference spectroscopy maintained in commercial spectroscopy or in public libraries.

The high sensitivity inherent in this technology allows efficient use of all device accessories such as reflection diffuser, total reflection attenuator, reflection polish attachment, and gas cells etc. that make FT-IR technology fast, versatile and reliable for characterization of materials [28].

Chapter Three

Experimental

3.1 Experimental

This part of the research includes a detailed description of the preparation of Aluminum Oxide (AL_2O_3), which is used to dope polystyrene (cork) dissolved in Benzene by the method of Sol-Gel method with volumetric ratios (0.1, to 0.9) mol with increasing step of 0.1 at a temperature Chamber by magnetic stirrer to obtain nine samples of doped polystyrene, and then studying the structural and optical properties of the samples by means of X-ray diffraction devices, a UV scale and an infrared device.

3.2 The Sol-Gel method

The sol-gel system consists of several locally available tools through which polystyrene can be doped, these are:

1- Magnetic stirrer and hot plate

2- Holder

3- Thermometer

4- Beakers

5- Sensitive balance

3.3 Preparation of Aluminum Oxide and Cork doping

For the preparation of Aluminum oxide , aluminum nitrate (AL $(NO3)_3 9H_2O)$) was used (as a source of Aluminum oxide, provided by (LOBA CHEMIE) company, with a molecular weight of 375.13 and a concentration of 98%, which is a white powder that is soluble in water, it was prepared at a temperature of (80) degrees Celsius for each Samples with different concentrations ranging from (0.1, 0.2, 0.3, 0.4, 0.5, 0.6, 0.7, 0.8, 0.9) %, by adding N, N- Dimethylformamide for HPLC and Spectroscopy as an simulating agent and precipitant, and through the following equations:

$$AL(NO_3)_3 9H_2O + H_2O \xrightarrow{\Delta} AL_2O_3 + H_2O$$

$$W_t = \frac{M_{wt} * V * M_{\mathrm{O}}}{1000}$$

Where

(M_{O}) Denotes the molecular concentration

(W_t) Denotes the

Solution weight

(M_{wt}) Denotes the molecular weight

(V) Denotes the volume of distilled water in (mL)

A (773 mg) was dissolved in (69 mL) of distilled water and placed in the magnetic stirrer at a temperature of 80^{o}c for 60 minutes, to obtain complete dissolution for the first sample, and then dissolve (740 mg) in (66.5 mL) of distilled water and placed in the magnetic stirrer at a temperature of 80^{o}c for 60 minutes to get the second sample. Also, (804 mg) was dissolved in (75 mL) of distilled water and placed in the magnetic stirrer at a temperature of 80^{o}c for 60 minutes to get the third sample, (761 mg) was dissolved in (68.5 mL) of distilled water and placed in the magnetic stirrer at a temperature of 80^{o}c for 60 minutes to obtain the fourth sample, then, (801 mg) was dissolved in (70 mL) of distilled water and placed in a magnetic stirrer at a temperature of 80^{o}c for 60 minutes to obtain the fifth sample, and (845 mg) was dissolved in (79 mL) of distilled water and placed in the magnetic stirrer at a temperature of 80^{o}c for 60 minutes to obtain the sixth sample, (744 mg) was dissolved in (66 mL) of distilled water and placed in a magnetic stirrer at a temperature of 80^{o}c for 60 minutes to obtain the seventh sample, and finally a (969 mg) was dissolved in (87 mL) of distilled water and placed in a magnetic stirrer at a temperature of 80^{o}c for 60 minutes to obtain the eighth sample, and (840 mg) was dissolved in (74 mL) of distilled water and placed in a magnetic stirrer at a temperature of 80^{o}c for 60 minutes to obtain the ninth sample.

Meanwhile, ten samples of the synthetic white cork (polystyrene) that was obtained after use (the waste) was dissolved in laboratory Benzene with a weight of 200 grams for each sample to become a solution and ten samples were prepared, to prepare doped cork samples, each of the nine previously prepared samples was added to a sample of 200 grams of cork dissolved in benzene and placed in the magnetic stirrer for 60 minutes to obtain the nine samples of the gelatinous solution of the cork doped by Aluminum oxide, then the solutions were placed in the bakers with the magnetic stirrer for 60 minutes to complete mixing and that to obtain a gelatinous solution. Spread it on glass slides, then leave the samples for 24 hours to dry and ready for testing

3.4 Optical Measurements

The study of the optical properties of materials is of great importance because it gives a lot of Information about the type of electronic transitions that occur in the material, in addition to leaving the energy beams; it also describes the properties that determine the interaction of light with matter.

When the energy of the radiation absorbed by the semiconductor is greater or equal, it is approximately to a value the energy gap (Eg), as it causes an electron to move from the valence beam filled with electrons to The conduction beam is devoid of electrons, so the area of the spectrum of the incident rays is defined and where it starts P are electrons moving at the absorption edge, and the amount differs in the energy between the lowest point in the conduction beam and the energy of the highest point in the valence beam is called the optical energy gap [6] Samples prepared and doped with aluminum oxide were tested by the UV device of Nelain University. The transmittance and absorption spectra were calculated for the wavelengths range from 400 to 800 nm, where the reflectivity,

absorption coefficient, extinction coefficient, refractive index and energy gap were calculated.

Fig 3.1 UV-Visible device

3.5. Structural Measurements

3.5.1 X-Ray Diffraction (XRD)

The structural properties are an important method for studying the crystal structure of layers, and this is done through the use of X-ray diffraction. X-ray diffraction analysis is used to know the nature of the crystal structure and the main crystalline phases, and that is to know the oriented direction of the prepared samples under certain conditions, as the general principle of diffraction depends on the phenomenon of interference that occurs when the movement of a wave is dispersed at a number of centers of atoms and as a result, either interference occurs constructive or destructive interference. polystyrene (cork) doped by aluminum oxide in different rate of molar (0.1, 0.2, 0.3, 0.4, 0.5, 0.6, 0.7,08, 0.9 and 1.0) are presented, the techniques of X-ray diffraction (XRD) was used to identify the precise crystal structure of the samples, where an X-ray was shed on the samples, which would appear according to reflections (Bragg) representing the atoms arranged in a specific direction, and through the data obtained from the tests of the prepared samples, the granular size,

lattice constants and density can be calculated, and macroscopic compliance, and the specifications of the X-ray diffraction device that was used at the University of Johannesburg – South Africa are as follows:

Type: XRD- 6000 Shimadzu

Target: Cu-Kα

Wave Length: 1.54060 °A

Speed: 5deg/min

Current: 30mA

Voltage: 40KV

3.5.2 Furrier transformation of infrared radiation

Fourier transform infrared spectrum (FTIR) is a technique used to obtain an infrared spectrum for the absorption or emission of a solid, liquid, or gas. The Fourier Spectrometer simultaneously collects spectral high-resolution data over a wide spectral range. This provides a major advantage over a spectrophotometer, which measures intensity over a narrow range of wavelengths simultaneously. The term infrared spectroscopy stems from the fact that a Fourier transform (a mathematical process) is required to convert the raw data to the actual spectrum. Other uses of this type of technology FTIR interference the central peak is in the ZPD position (Zero path difference or zero delay) with the maximum amount of light passing through the interferometer to the detector.

Chapter Four

Results and Discussion

4.1 Interdiction

In this part of the research, the main results that have been obtained from the experiments made of (polystyrene (cork) doped by aluminum oxide) in different rate of molar (0.1, 0.2, 0.3, 0.4, 0.5, 0.6, 0.7,08, 0.9) Molar are presented. The data of X-ray diffraction (XRD) have been analyzed to ensure good quality of the samples (their crystal structure, their lattice parameters, the positions of atoms within the cell), the FT-IR data have been carried to investigate the chemical bonds within atoms and the data of UV-visible used to evaluate the band gap and optical properties.

4.2 Optical Results of (Polystyrene (cork) doping by Aluminum Oxide)) samples

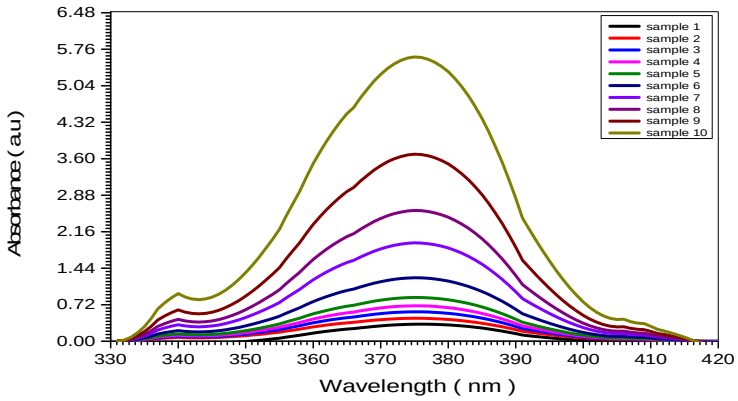

Fig(4.1) Relation between absorbance and wavelengths of polystyrene(cork) doping by aluminum oxide in different rate of molar (0.1 ,0.2 ,0.3 ,0.4 ,0.5 ,0.6 ,0.7,08 ,0.9 and 1.0)

In the absorbance graph we found that the behavior of the curves is the same for the ten samples of polystyrene (cork) doped by aluminum oxide in different rate of molar (0.1, 0.2, 0.3, 0.4, 0.5, 0.6, 0.7,08, 0.9 and 1.0)

studied. Using UV-VIS 1240 min spectrophotometer, showed all the results of absorbance in fig (4.1). Fig. (4.1) shows the relation between absorbance and wavelengths for polystyrene (cork) doped by aluminum oxide in different rate of molar which gives gradually increasing in the a absorption up to the wavelengths 375 nm at which crosponding to the photon energy 3.31 eV, and that is directly proportional to the doping rate of the (aluminum oxidemolar).

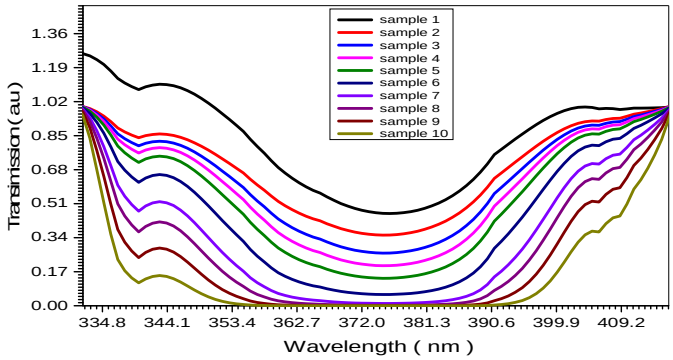

Fig(4.2) Relation between transsimitance and wavelengths of polystyrene (cork) doped by aluminum oxide in different rate of molar (0.1 ,0.2 ,0.3 ,0.4 ,0.5 ,0.6 ,0.7,08 ,0.9 and 1.0)

In the transmittance graph we found the that the behavior of curves is the same for polystyrene (cork) doped by aluminum oxide in different rate of molar (0.1 ,0.2 ,0.3 ,0.4 ,0.5 ,0.6 ,0.7,08 ,0.9 and 1.0) samples, Fig. (4.2) shows the efficet of doping on the transmittance and it clarifyed an inverse proportional between the doping rate and the transmittance value.

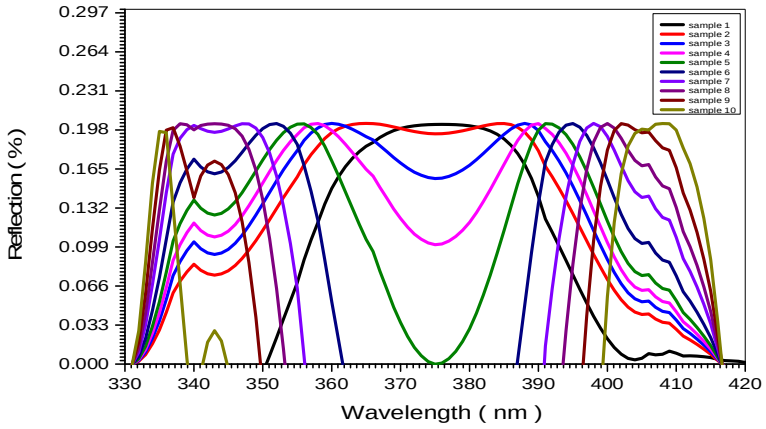

Fig(4.3) relation between reflection and wavelengths of polystyrene (cork) doped by aluminum oxide in different rate of molar (0.1 ,0.2 ,0.3 ,0.4 ,0.5 ,0.6 ,0.7,08 ,0.9 and 1.0) samples

The reflection graph for all samples of polystyrene (cork) doped by aluminum oxide in different rate of molar (0.1 ,0.2 ,0.3 ,0.4 ,0.5 ,0.6 ,0.7,08 ,0.9 and 1.0) is presented in fig. (4.3), which shows that the reflection for all samples of polystyrene (cork) doped by aluminum oxide in different rate of molar has a maximum value of 0.1972 % in the wave length range (335 to 410) nm, at this range the reflection becomes completely a mirror. The efficet of doping on the refelection increases the transission by increasing the dopping rate, and the graph shefted towards the red spectrum after the wave length value of 375 nm and plue sheft befor 375 nm.

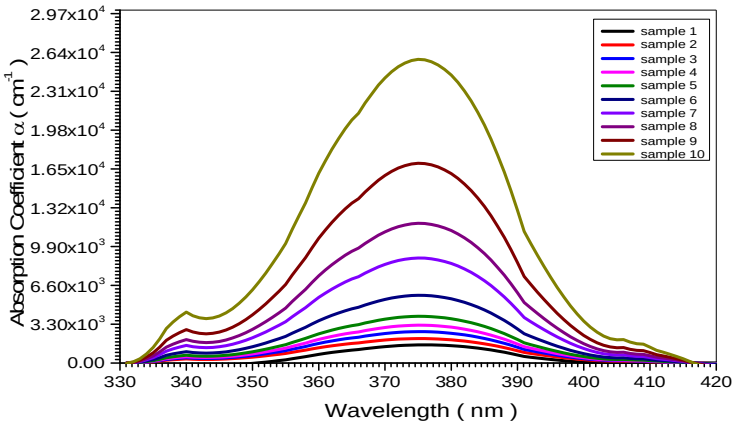

Fig(4.4): The relation between absorption coefficient and wavelengths of polystyrene (cork) doped by aluminum oxide in different rate of molar (0.1 ,0.2 ,0.3 ,0.4 ,0.5 ,0.6 ,0.7,08 ,0.9 and 1.0)

The absorption coefficient (α) of all polystyrene (cork) doped by aluminum oxide in different rate of molar (0.1 ,0.2 ,0.3 ,0.4 ,0.5 ,0.6 ,0.7,08 ,0.9 and 1.0) was found from equation (5). Fig (4.4) shows the plot of (α) vrs wavelength (λ) of polystyrene (cork) doped by aluminum oxide in different rate of molar, and obtained that the value of $\alpha = 1.55x10^3$ cm^{-1} for sample 1 in the U.V region(375 nm) but for sample 10 it equal $2.58x10^4$ cm^{-1} at the same wavelength, that means the transition must corresponds to a direct electronic transition, and the properties of this state are important since they are responsible of the electrical conductivity. Also, fig.(4.4) shows that the value of (α) for the all polystyrene (cork) doped by aluminum oxide in different rate of molar increases while doing rate increases in a direct proportionality.

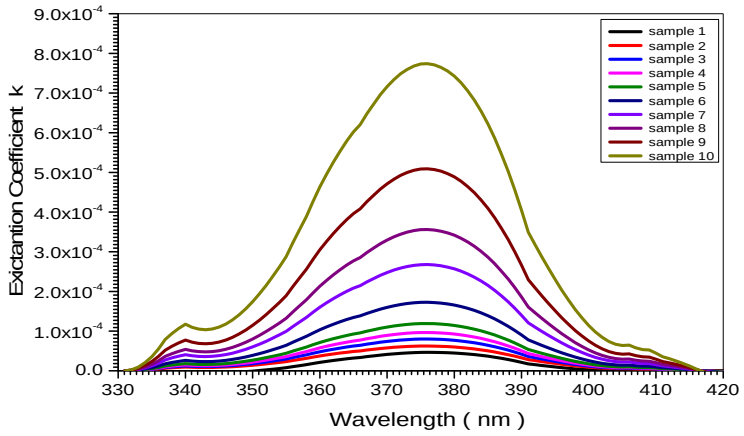

Fig (4.5) the relation between extinction coefficient and wavelengths of polystyrene (cork) doped by aluminum oxide in different rate of molar (0.1, 0.2, 0.3, 0.4, 0.5, 0.6, 0.7,08, 0.9 and 1.0)

Extinction coefficient (K) was calculated using the equation $K = \frac{\alpha\lambda}{4\pi}$ The variation at the (K) values as a function of (λ) is shown in fig (4.5) for all polystyrene (cork) doped by aluminum oxide in different rate of molar (0.1, 0.2, 0.3, 0.4, 0.5, 0.6, 0.7,08, 0.9 and 1.0) samples and it is observed that the spectrum shape of (K) is the same as that of (α). The Extinction coefficient (K) for all polystyrene (cork) doped by aluminum oxide in different rate of molar samples showed the value of (K) at (375 nm) wavelength, depending on the samples treatment method, where the value of (K) at 250 nm for sample 1 equal 4.45×10^{-5} while for sample 10 at the same wavelength equal 7.75×10^{-4}. The effect of aluminum oxide in different rate of molar occurs as a direct proportional, in other words, increasing the aluminum oxide doping rate causes increasing the Extinction coefficient (k) value.

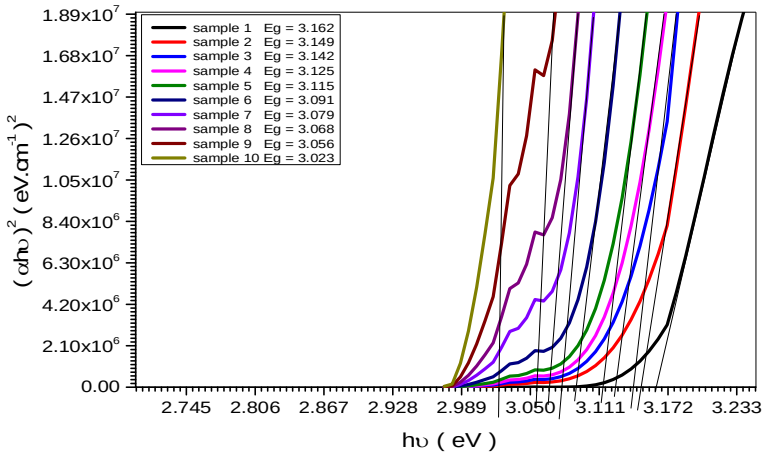

Fig(4.6) the relation between the optical energy band gap of all polystyrene (cork) doped by aluminum oxide in different rate of molar (0.1 ,0.2 ,0.3 ,0.4 ,0.5 ,0.6 ,0.7,08 ,0.9 and 1.0) and the photon energy

The optical energy gap (Eg) has been calculated via equation $(\alpha h\upsilon)^2 = C(h\upsilon - Eg)$ where (C) is constant. Plotting $(\alpha h\upsilon)^2$ vrs photon energy $h\upsilon$ is shown in fig (4.6) for all polystyrene (cork) doped by aluminum oxide in different rate of molar (0.1 ,0.2 ,0.3 ,0.4 ,0.5 ,0.6 ,0.7,08 ,0.9 and 1.0) samples. And by extra polating the straight thin tangant of the curve to intercept the energy axis, the value of the energy gap has been calculated for sample (1) and found to be equal (3.162) eV while for sample (10) is equal to (3.023) eV. The value of (Eg) was decreased from (3.162) eV to (3.023) eV, the decreasing of (Eg) related to increasing of aluminum oxide dopping rate of the samples. It was observed that the different aluminum oxide rate of molar confirmed the reason for the band gap shifts.

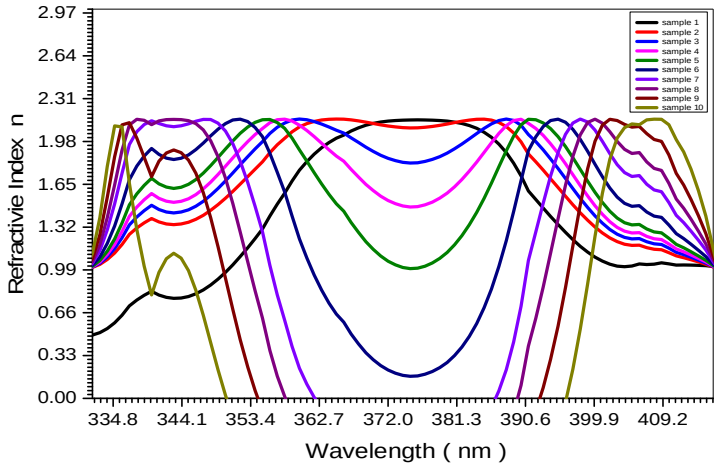

Fig(4.7) the relation between refactivie index and wavelengths of polystyrene (cork) doped by aluminum oxide in different rate of molar (0.1 ,0.2 ,0.3 ,0.4 ,0.5 ,0.6 ,0.7,08 ,0.9 and 1.0)

The refractive index (n) is the relative between speed of light in vacuum to its speed in material which does not absorb this light. The value of n was calculated from the equation $n = \left[\left(\frac{1+R}{1-R}\right)^2 - \left(k_0^2 + 1\right)\right]^{\frac{1}{2}} + \frac{1+R}{1-R}$, Where (R) is the reflectivity. The variation of (n) vrs (λ) for all polystyrene (cork) doped by aluminum oxide in different rate of molar (0.1 ,0.2 ,0.3 ,0.4 ,0.5 ,0.6 ,0.7,08 ,0.9 and 1.0) is shown in fig (4.7). Fig (4.7) Show the plot of the refractive index (n) spectra of all polystyrene (cork) doped by aluminum oxide in different rate of molar, which indicates that the maximum value of (n) is (2.145) for all samples at wavelength ranged (335 to 410) nm, which is agree with the red shift that take place for aluminum oxide doping rate byond the wavelength 375 nm , and blue the shift befor the wavelength 375 nm on the spectrum

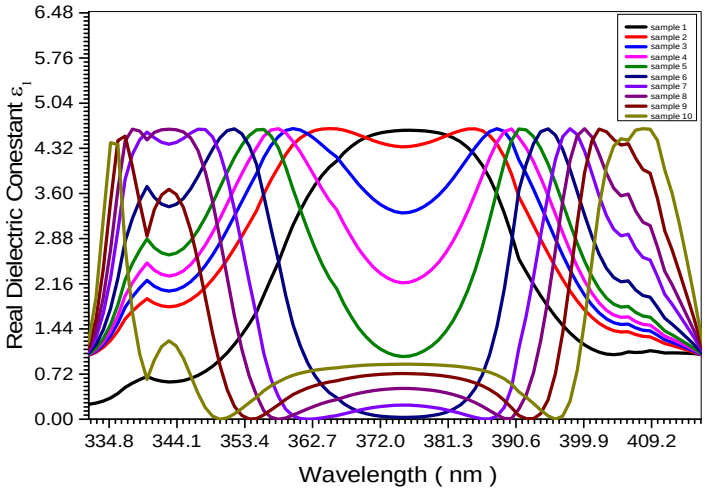

Fig (4.8) the relation between the real dielectric constant and wavelengths of polystyrene (cork) doped by aluminum oxide in different rate of molar (0.1 ,0.2 ,0.3 ,0.4 ,0.5 ,0.6 ,0.7,08 ,0.9 and 1.0)

Fig (4.8) shows the variation of the real dielectric constant (ε_1) with the wavelength of all samples prepared by polystyrene (cork) doped by aluminum oxide in different rate of molar, which calculatedfrom the relation $\varepsilon_1 = n^2 - k^2$ Where the real the dielectric constant (ε_1) is the normal dielectric constant. From fig (4.8) the variation of (ε_1) followed the refractive index, where at wavelength ranged (335 to 410) nm for all samples of polystyrene (cork) doped by aluminum oxide in different rate of molar, the absorption of the samples at these wavelength is small, but the polarization increased, and the maximum value of (ε1) equal to (4.63) at wavelength 375 nm. The effect of the treatment by aluminum oxide in different rate of molar of the samples on the (ε1) is shifted towards the red spectrum befor 375 nm and shifted towards the blue spectrum after 375 nm

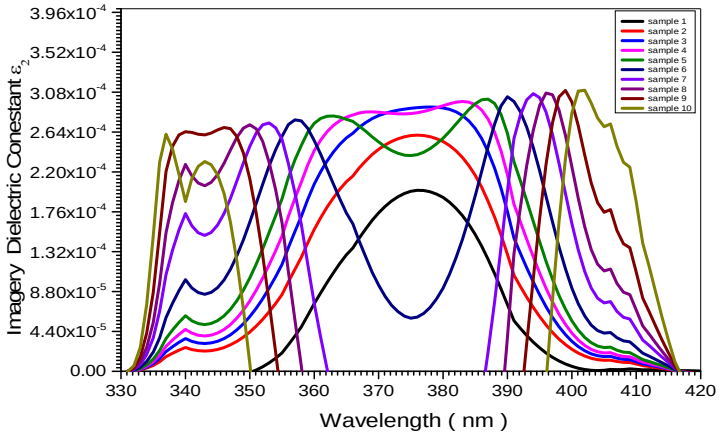

Fig(4.9) the relation between imaginary dielectric conestant and wavelengths of polystyrene (cork) doped by aluminum oxide in different rate of molar (0.1 ,0.2 ,0.3 ,0.4 ,0.5 ,0.6 ,0.7,08 ,0.9 and 1.0)

Fig (4.9) shows the variation of the Imagery dielectric constant (ε_2) with wavelength of all samples prepared by polystyrene (cork) doped by aluminum oxide in different rate of molar, which calculated from the relation $\varepsilon_2 = 2nk$ Where the imaginary dielectric constant (ε_2) is the up-normal dielectric constant. From fig (4.9) the variation of (ε_2) is follows the refractive index, where at wavelength ranged (335 to 410) nm for all samples of polystyrene (cork) doped by aluminum oxide in different rate of molar the maximum value of (ε_2) equal to (2.91×10^{-4}) at wavelength 375 nm, and the effect of the treatment by aluminum oxide in different rate of molar of the samples on the (ε2) is shifted towards the red spectrum befor 375 nm and shifted towards the blue spectrum after 375 nm .

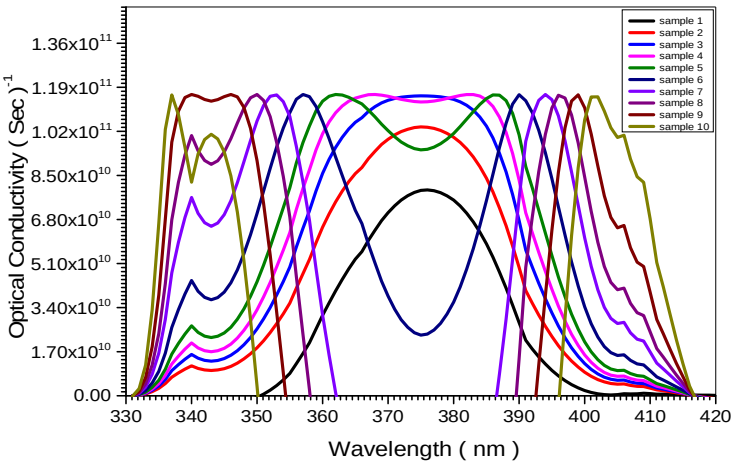

Fig(4.10) the relation between optical conductivity and wavelengths of polystyrene (cork) doping by aluminum oxide in different rate of molar (0.1 ,0.2 ,0.3 ,0.4 ,0.5 ,0.6 ,0.7,08 ,0.9 and 1.0).

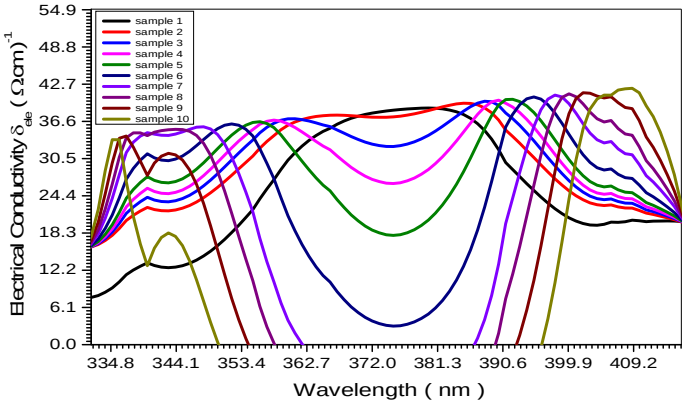

Fig(4.11) the relation between electrical conductivity and wavelengths of polystyrene (cork) doping by aluminum oxide in different rate of molar (0.1 ,0.2 ,0.3 ,0.4 ,0.5 ,0.6 ,0.7,08 ,0.9 and 1.0).

Electrical and Optical Conductivity: The optical conductivity is a measure of frequency response of the material when irradiated with light which is determined using the following relation, $\delta_{opt} = \frac{\alpha n c}{4\pi}$ Where (c) is the light velocity. The electrical conductivity can be estimated using the following relation $\delta_{ele} = \frac{2\lambda\delta_{opt}}{\alpha}$. The high magnitude of optical conductivity ($1.66x10^{11}$ sec^{-1}) confirms the presence of a very high photon response of the all polystyrene (cork) doped by aluminum oxide

in different rate of molar. The increasing of optical conductivity at high photon energies is due to the high absorbance of polystyrene (cork) doped by aluminum oxide in different rate of molar, and may be due to electron excitation by photon energy as it is shown in Figs (4.10) and (4.11).

4.3 XRD Results of (Polystyrene (cork) doped by Aluminum Oxide) samples

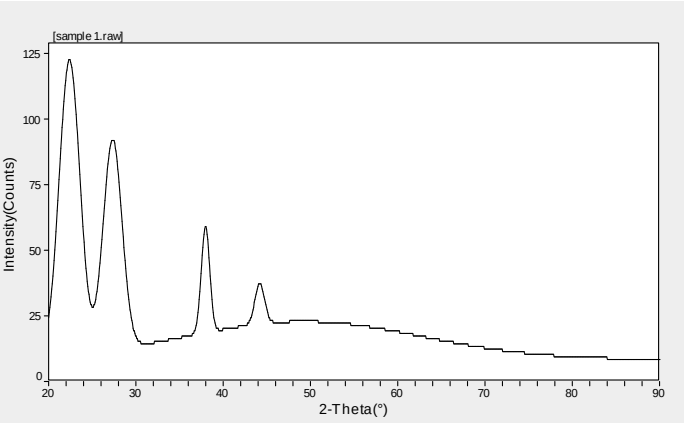

Fig (4.12) XRD spectrum of sample1

Table (4.1) Calculate Lattice Constants from Peak Locations and Miller Indices [Monoclinic] of sample1

2Θ	d (nm)	h k l	X_s (nm)
22.869	3.8855	3 1 1	6.2
27.781	3.2086	4 1 1	15.2
37.974	2.3675	1 3 0	9.9

Cell Volume = 123.3 $(A^O)^3$

a= 10.277 b =12.66 c = 10.629

$\alpha = 90^O \beta = 116.82^O \gamma = 90^O$

Density = 7.8117mg.cm^{-3}

Crystal Form: Monoclinic – Primitive

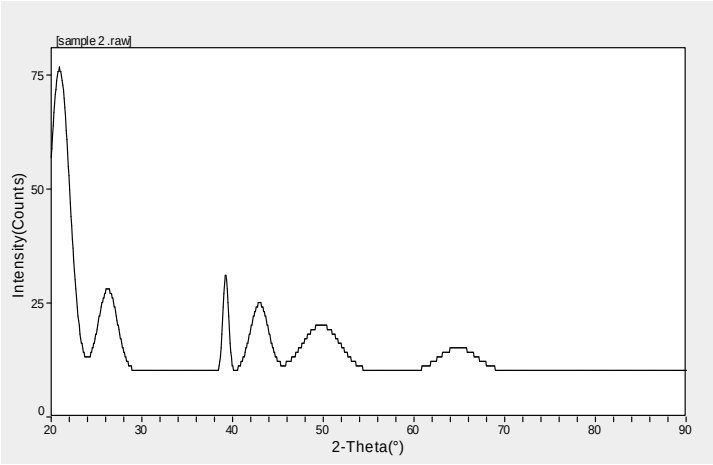

Fig (4.13) XRD spectrum of sample 2

Table (4.2) Calculate Lattice Constants from Peak Locations and Miller Indices [Tetragonal] of sample 2

2Θ	d (nm)	h k l	X_s (nm)
39.21	22.957	1 1 2	14.3

Cell Volume = 126.3 $(A^O)^3$

a= b = 3.842 c = 8.553

$\alpha = \beta = \gamma = 90^O$

Density = 6.8865 $mg.cm^{-3}$

Crystal Form: Tetragonal – I- Center

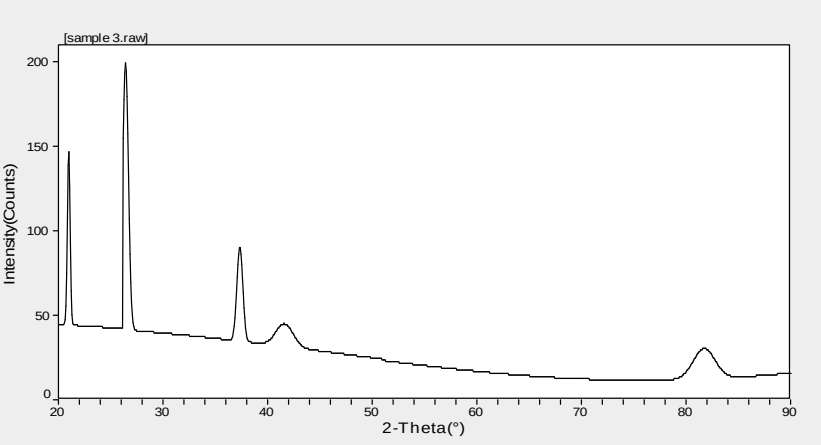

Fig (4.14) XRD spectrum of sample 3

Table (4.3) Calculate Lattice Constants from Peak Locations and Miller Indices [Monoclinic] of sample3

2Θ	d (nm)	h k l	X_s (nm)
20.972	4.2325	0 0 2	30.2
26.324	3.3828	2 1 1	18.3
37.363	2.4048	3 1 1	14.7

Cell Volume = 492 $(A^O)^3$

a= 7.605 b =7.754 c = 8.627

$\alpha = 90^O \beta = 104.6^O \gamma = 90^O$

Density = 5.2817mg.cm^{-3}

Crystal Form: Monoclinic– Primitive

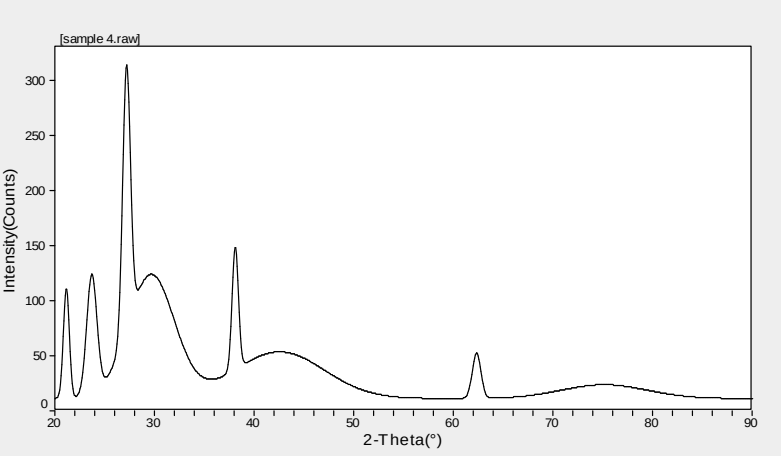

Fig (4.15) XRD spectrum of sample4

Table (4.4) Calculate Lattice Constants from Peak Locations and Miller Indices [Triclinic] of sample 4

2Θ	d (nm)	h k l	X_s (nm)
21.14	4.1911	1 1 2	12.6
23.734	3.47458	0 2 3	8.0
38.022	2.3646	1 3 3	12.3

Cell Volume = $540.6(A^O)^3$

a=6.9804 b =8.7402 c = 10.283

$\alpha = 107.702^O \beta = 105.269^O \gamma = 103.881^O$

Density = $4.997 mg.cm^{-3}$

Crystal Form: Triclinic – Primitive

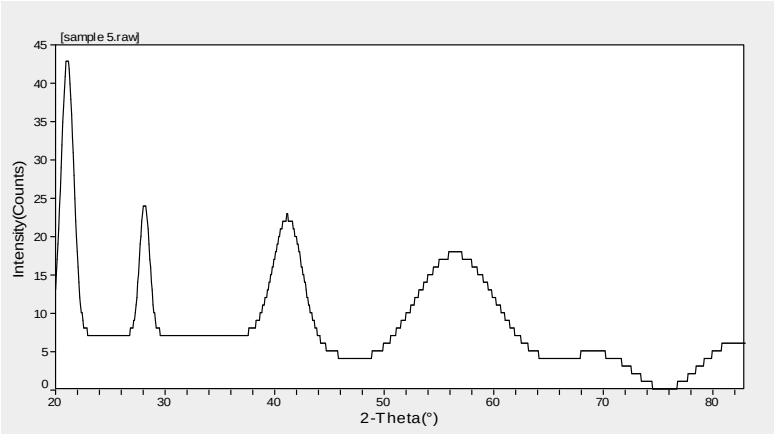

Fig (4.16) XRD spectrum of sample5

Table (4.5) Calculate Lattice Constants from Peak Locations and Miller Indices [Monoclinic] of sample 5

2Θ	d (nm)	h k l	X_s (nm)
21.037	4.2194	1 2 1	8.1

Cell Volume = 1126.2 $(A^O)^3$

a=7.353 b =25.225 c = 6.097

$\alpha = 90^O \beta = 95.2^O \gamma = 90^O$

Density = 4.0653mg.cm^{-3}

Crystal Form: Monoclinic – Primitive

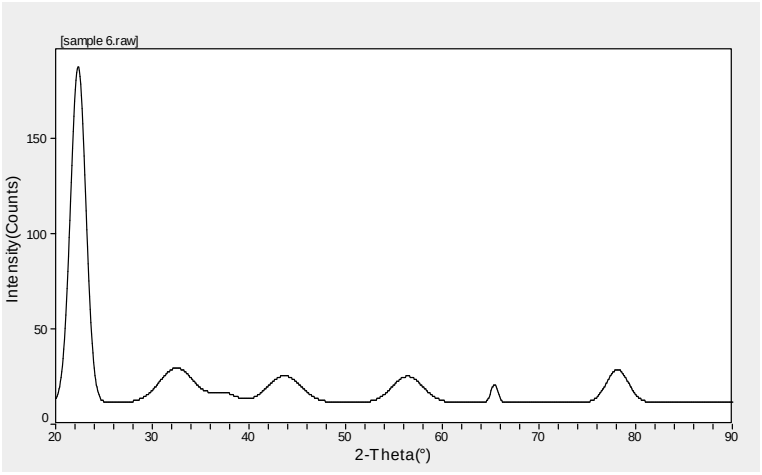

Fig (4.17) XRD spectrum of sample 6

Table (4.6) Calculate Lattice Constants from Peak Locations and Miller Indices [Hexagonal] of sample 6

2Θ	d (nm)	h k l	X_s (nm)
22.321	3.9795	2 1 1	7.7

Cell Volume = 1385.5 $(A^O)^3$

a= 13.74 b = 13.74 c = 8.474

$\alpha = 90\ ^O\beta = 90\ ^O\gamma = 120^O$

Density = 4.0001 $mg.cm^{-3}$

Crystal Form: Hexagonal – Primitive

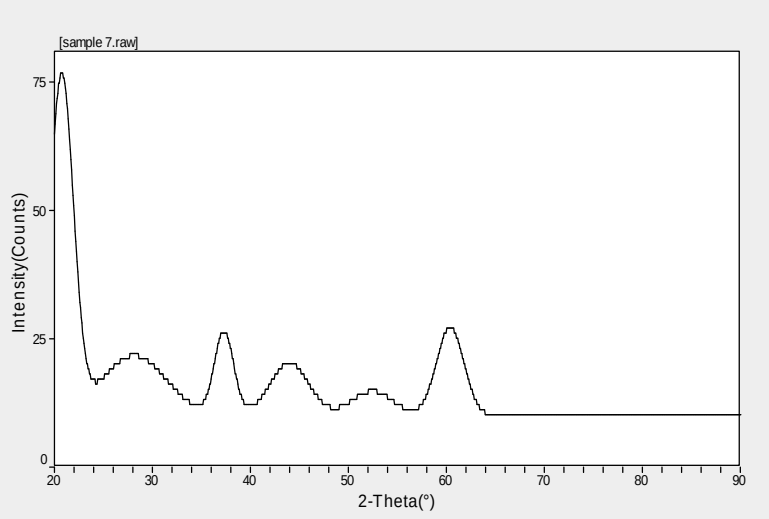

Fig (4.18) XRD spectrum of sample7

Table (4.7) Calculate Lattice Constants from Peak Locations and Miller Indices [Hexagonal] of sample 7

2Θ	d (nm)	h k l	X_s (nm)
22.321	3.9795	2 1 1	7.7

Cell Volume = 1385.5 $(A^O)^3$

a= 13.74 b = 13.74 c = 8.474

$\alpha = 90\ ^O\beta = 90\ ^O\gamma = 120^O$

Density = 4.0001 $mg.cm^{-3}$

Crystal Form: Hexagonal – Primitive

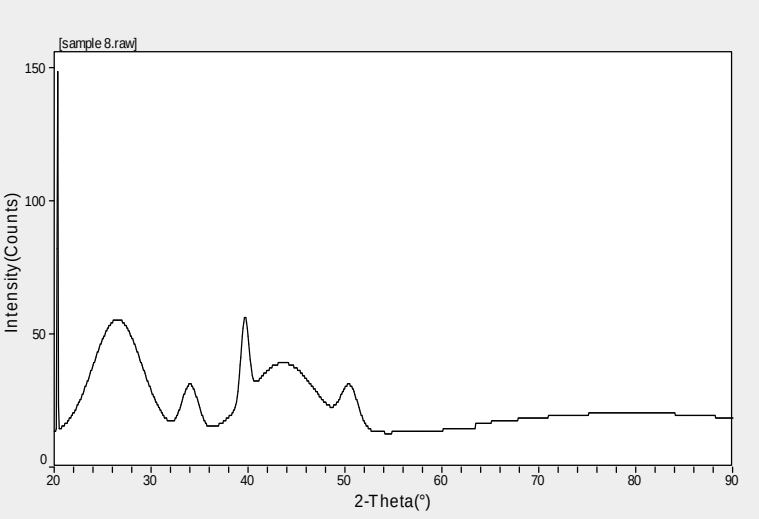

Fig (4.19) XRD spectrum of sample8

Table (4.8) Calculate Lattice Constants from Peak Locations and Miller Indices [Orthorhombic] of sample 8

2Θ	d (nm)	h k l	X_s (nm)
39.65	2.2713	0 2 3	12.9

Cell Volume = 613.4$(A^O)^3$

a=5.9436b =14.433c = 7.1508

$\alpha = 90\ ^O\beta = 90\ ^O\gamma = 90^O$

Density = 3.5508mg.cm^{-3}

Crystal Form: Orthorhombic – C-Center

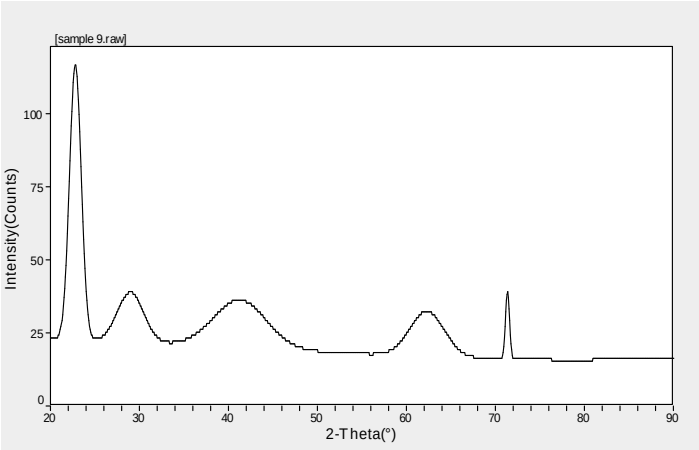

Fig (4.20) XRD spectrum of sample 9

Table (4.9) Calculate Lattice Constants from Peak Locations and Miller Indices [Monoclinic] of sample 9

2Θ	d (nm)	h k l	X_s (nm)
22.764	3.9031	2 2 2	6.4
73.44	1.3208	1 5 0	20

Cell Volume = 22594.9 $(A^O)^3$

a= 14.044 b = 13.812 c = 13.382

$\alpha = 90\ ^O\beta = 91.48\ ^O\gamma = 90^O$

Density = 2.3003 $mg.cm^{-3}$

Crystal Form: Monoclinic – Primitive

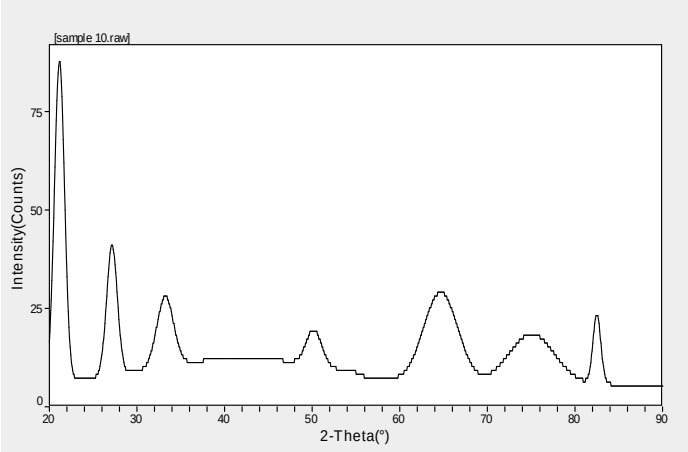

Fig (4.21) XRD spectrum of sample 10

Table (4.10) Calculate Lattice Constants from Peak Locations and Miller Indices [Monoclinic] of sample 10

2Θ	d (nm)	h k l	X_s (nm)
21.295	4.1689	0 2 0	7.6
27.358	3.2572	2 1 1	6.3

Cell Volume = 492.5 $(A^O)^3$ a=11.045b =8.193c = 5.535

$\alpha = 90\ ^O\beta = 100.5^O\gamma = 90^O$Density = 1.4873 $mg.cm^{-3}$

Crystal Form: Monoclinic – Primitive

Table (4.11) some crystallite lattice parameter (c- form, density, Xs (nm) and d – spacing) of polystyrene (cork) doping by aluminum oxide samples

No	Crystal Form	Density ($mg.cm^{-3}$)	Cell Volume $(A^{O})^{3}$	d (nm)	X (nm)
1	Monoclinic-Primitive	7.8117	123.3	2.15386	17.483
2	Tetragonal–I- Center	6.90469	126.3	2.29	15.501
3	Monoclinic–Primitive	5.9817	492	2.6713	13.66
4	Triclinic – Primitive	5.38433	540.6	2.7119	12.57
5	Monoclinic–Primitive	4.53865	1126.2	3.343	11.23
6	Hexagonal–Primitive	4.01859	1385.5	3.443	10.32
7	Hexagonal–Primitive	3.42123	1385.5	3.575	9.599
8	Orthorhombic–C-Center	2.86369	613.4	3.713	8.72
9	Monoclinic–Primitive	2.18902	22594.9	3.9795	7.85
10	Monoclinic–Primitive	1.4873	492.5	4.2194	6.95

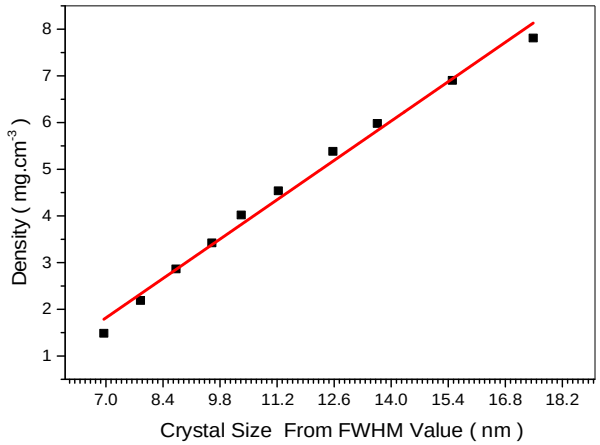

Fig (4.22) relation sheep between Crystal size and density of polystyrene (cork) doping by aluminum oxide in different rate of molar (0.1 ,0.2 ,0.3 ,0.4 ,0.5 ,0.6 ,0.7,08 ,0.9 and 0.10) Molarsamples

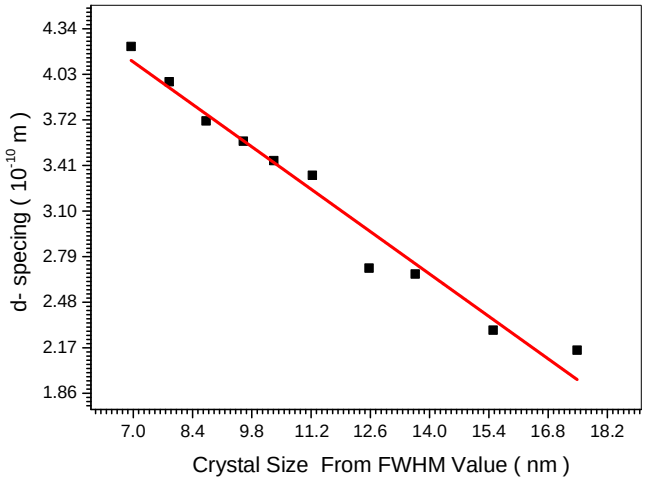

Fig (4.23) relation sheep between Crystal size and d- spacing of polystyrene (cork) doping by aluminum oxide in different rate of molar (0.1, 0.2, 0.3, 0.4, 0.5, 0.6, 0.7,08, 0.9 and 1.0) Molar samples

The crystal structure of all samples characterized at room temperature using a Philips PW1700 X-ray diffractometer (operated at 40 kV and current of 30 mA) and samples were scanned between 20^{O} and 90^{O} at a scanning speed of 0.06 ^{o}C/s using Cu Kα radiation with λ = 1.5418Å. The representative XRD charts of all polystyrene (cork) doping by aluminum

oxide in different rate of molar (0.1 ,0.2 ,0.3 ,0.4 ,0.5 ,0.6 ,0.7,08 ,0.9 and 0.10) Molar samples as show in fig (4.12) to fig (4.23). Miller indices provided in the figure and all peaks determine transformation of polystyrene (cork) doping by aluminum oxide in different rate of molar (0.1 ,0.2 ,0.3 ,0.4 ,0.5 ,0.6 ,0.7,08 ,0.9 and 0.10) Molarsamplescrystallites with tetragonal rutile crystal structure. Table (4.1) to table (4.11) shows the XRD parameters of polystyrene (cork) doping by aluminum oxide at various crystalline orientations. Fig (4.22) describes the relation between the Crystal size of polystyrene (cork) doping by aluminum oxide samples and density of samples, we showing that increase the density of sample by increasing the Crystal size samples by rat (0.60234 mg. cm^{-3}/nm). The dislocation density (δ) and number of unit cells (n) of polystyrene (cork) doping by aluminum oxide in different rate of molar (0.1 ,0.2 ,0.3 ,0.4 ,0.5 ,0.6 ,0.7,08 ,0.9 and 0.10) Molarsamplesnanoparticles is calculated and listed in table (4.11). Dislocation density decreases and the by number of unit cells increases growth and decreasing the defects in crystallites. Finally, fig (4.23) describes the relation between the read Crystal size of polystyrene(cork) doping by aluminum oxide samples and d- spesing of polystyrene(cork) doping by aluminum oxide in different rate of molar (0.1 ,0.2 ,0.3 ,0.4 ,0.5 ,0.6 ,0.7,08 ,0.9 and 0.10) Molarnanoparticles samples, and noticed that the rated of decreasing the d- spesing of polystyrene(cork) doping by aluminum oxide samples with increases the Crystal size $0.2061x10^{-10}$m / nm.

4.4FTIR Results of (Polystyrene (cork) doping by Aluminum Oxide)) samples

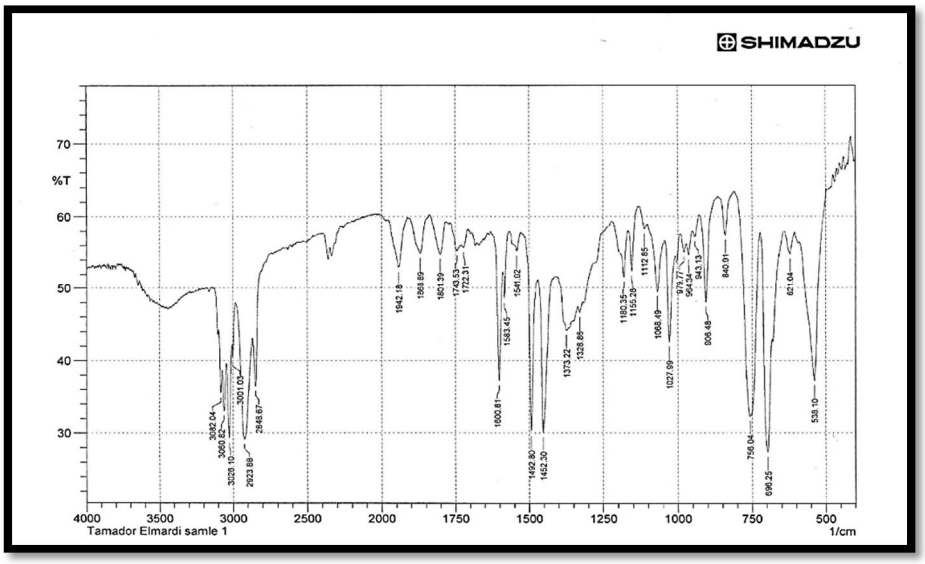

Fig (4.24) FTIR spectrum of sample 1 for polystyrene(cork)

Table (4.12) FTIR wave number of sample 1 for polystyrene (cork)

Wave length(cm^{-1})	Symbol and Bond	Function group
545	C-H	Mono
700	C-H	Mono
750	C-H	Ortho distributer aromatic
1025	C-O	Stretch
1450	C=C	Stretch (isolated)
1500	N=O	Aliphatic
2900	C-H	Stretch
3000	C-H	Stretch alkynes
1650	C=O	Stretch ketones

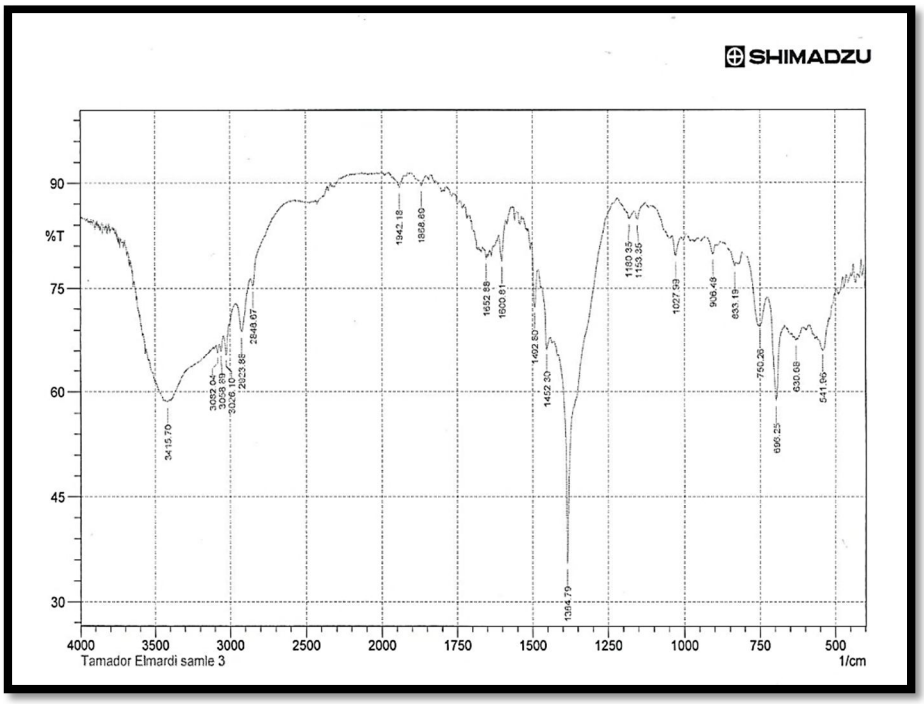

Fig (4.25) FTIR spectrum of sample 2 for polystyrene(cork) doping by aluminum oxide

Table (4.13) FTIR wavenumber of sample 2 for polystyrene (cork) doping by aluminum oxide

Wave length(cm^{-1})	Symbol and bond	Function group
520	AL_2O_3	Metallic oxide
700	AL_2O_3	Metallic oxide
1375	N=O	Nitro symmetric
2950	C-H	Stretch
3450	O-H	Water

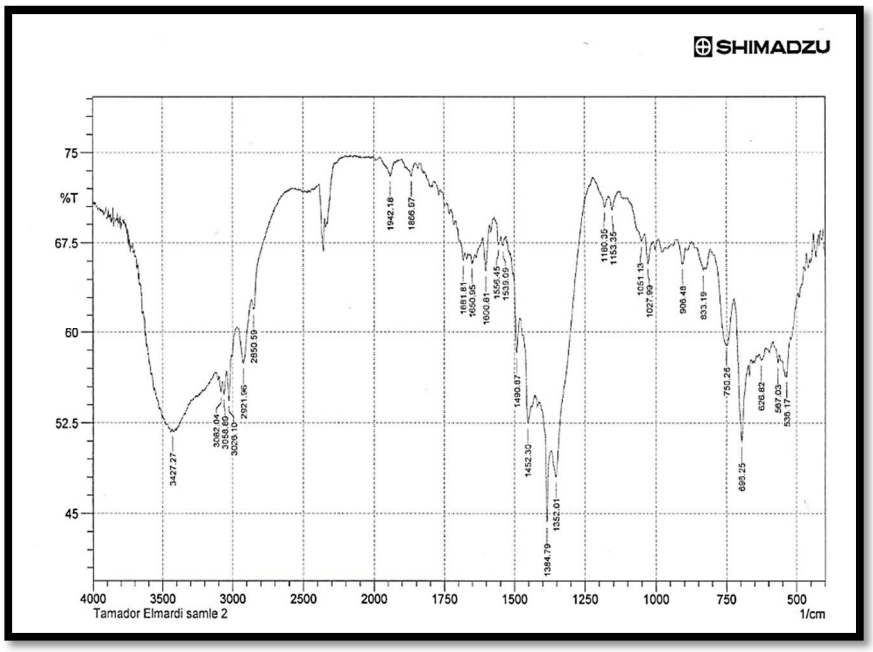

Fig (4.26) FTIR spectrum of sample 3 for polystyrene(cork) doping by aluminum oxide

Table (4.14) FTIR wavenumber of sample 3 for polystyrene (cork) doping by aluminum oxide

Wave length(cm^{-1})	Symbol and Bond	Function group
550	AL_2O_3	Metallic oxide
600	C-H	Mono substituted aromatic
1390	N-O	Aromatic
1650	C=O	Amides saturated
3450	O-H	Water

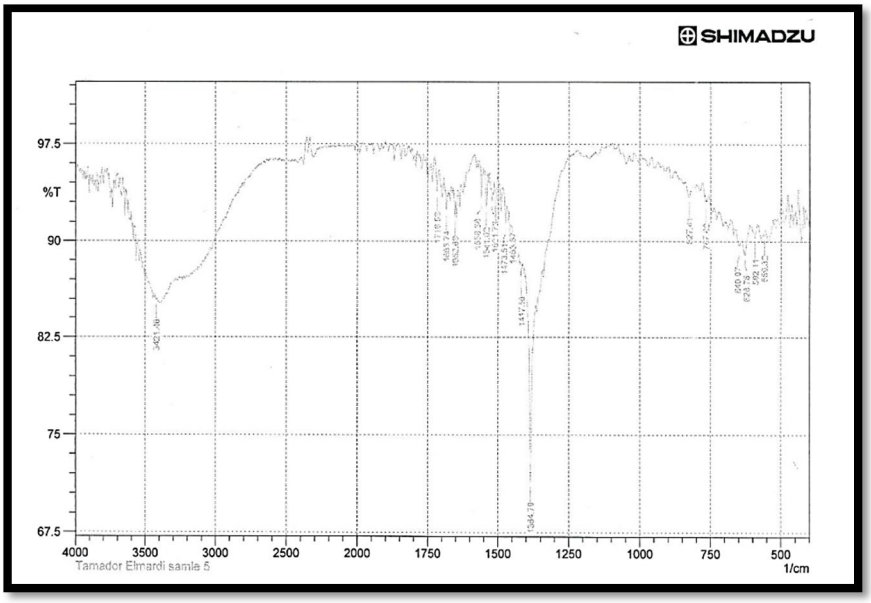

Fig (4.27) FTIR spectrum of sample 4 for polystyrene(cork) doping by aluminum oxide

Table (4.15) FTIR wavenumber of sample 4 for polystyrene (cork) doping by aluminum oxide

Wave length(cm^{-1})	Symbol and Bond	Function group
690	C-H	Mono substituted aromatic
1385	N-O	Nitro symmetric
1700	C=O	Stretch
3300	CΞC	Stretch

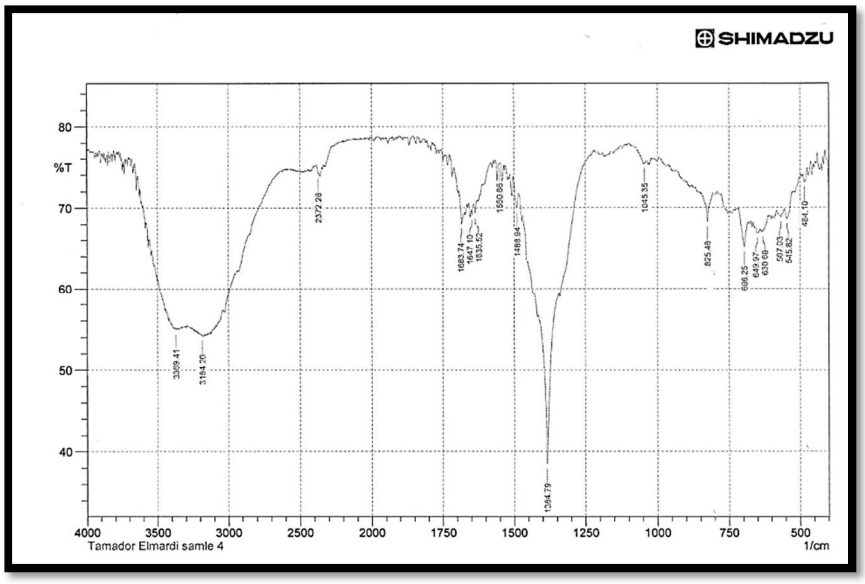

Fig (4.28) FTIR spectrum of sample 5 for polystyrene(cork) doping by aluminum oxide

Table (4.16) FTIR wavenumber of sample 5 for polystyrene (cork) doping by aluminum oxide

Wave length(cm^{-1})	Symbol and Bond	Function group
650	C-H	Mono
1357	N=O	Symmetric
1650	C=O	Esters
3400	O-H	Water

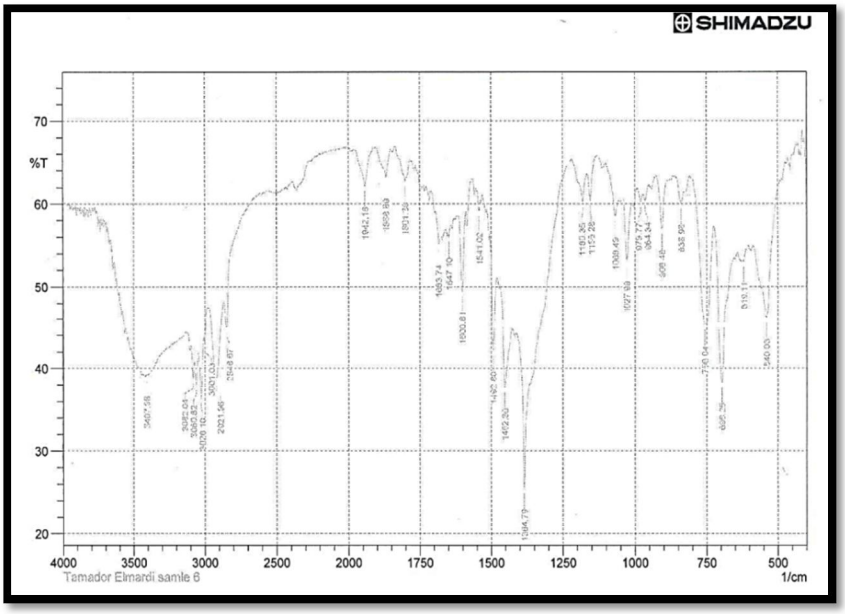

Fig (4.29) FTIR spectrum of sample 6 for polystyrene(cork) doping by aluminum oxide

Table (4.17) FTIR wavenumber of sample 6 for polystyrene (cork) doping by aluminum oxide

Wave length(cm^{-1})	Symbol and Bond	Function group
550	AL_2O_3	Metallic oxide
700	AL_2O_3	Metallic oxide
1045	C-N	Stretch (alkyl)
1400	C-H	In plane bend
1650	C=O	Amides saturated
3000	C-H	Carboxylic acid
3400	O-H	Water

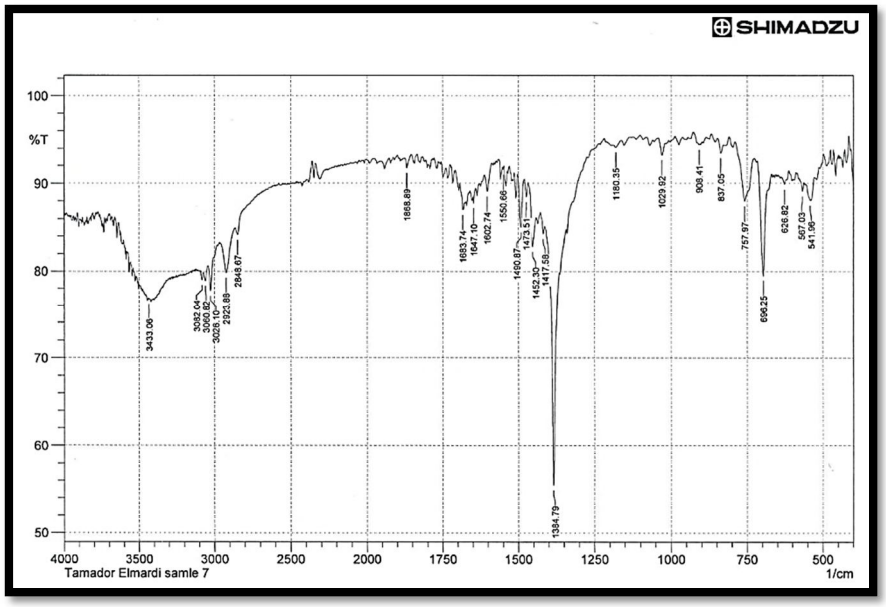

Fig (4.30) FTIR spectrum of sample 7 for polystyrene(cork) doping by aluminum oxide

Table (4.18) FTIR wavenumber of sample 7 for polystyrene (cork) doping by aluminum oxide

Wave length(cm^{-1})	Symbol and Bond	Function group
525	AL_2O_3	Metallic oxide
700	AL_2O_3	Metallic oxide
1375	N-O	Nitro symmetric
1685	C=N	Stretch
3000	C-H	Carboxylic acid
3425	C-N	Amides and amines

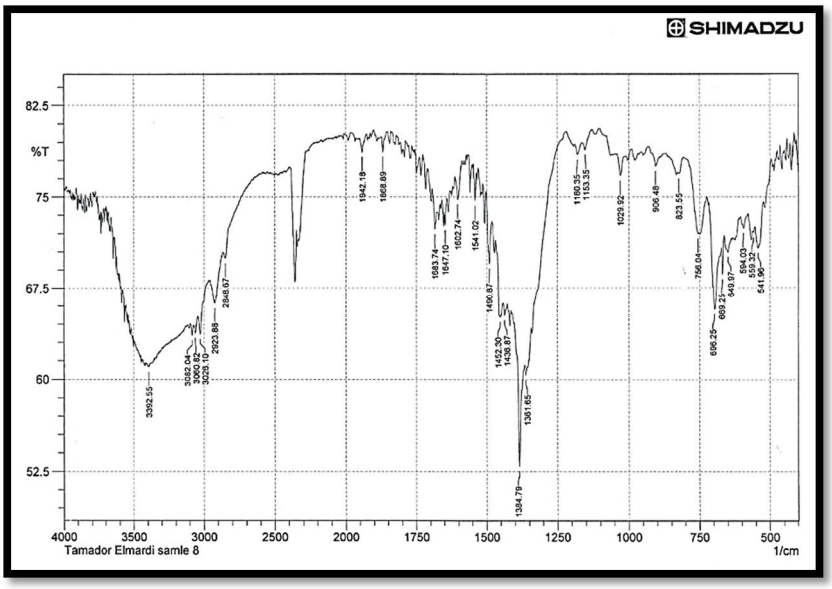

Fig (4.31) FTIR spectrum of sample 8 for polystyrene(cork) doping by aluminum oxide

Table (4.19) FTIR wavenumber of sample 8 for polystyrene (cork) doping by aluminum oxide

Wave length(cm^{-1})	symbol and Bond	Function group
520	AL_2O_3	Metallic oxide
700	AL_2O_3	Metallic oxide
1385	N-O	Nitro symmetric
1700	C=O	Stretch ketones
2950	C-H	Aldehyde stretch
3400	O-H	Water

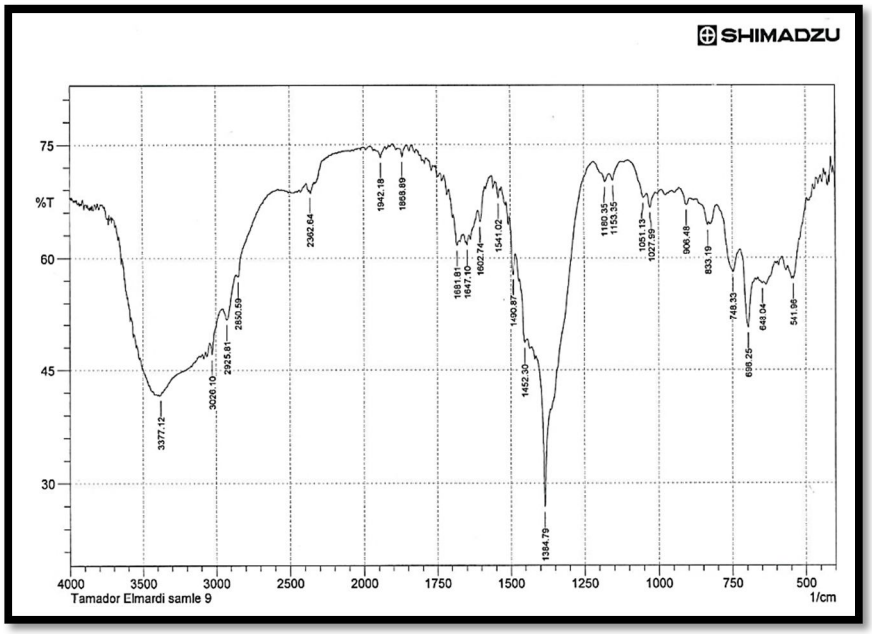

Fig (4.32) FTIR spectrum of sample 9 for polystyrene(cork) doping by aluminum oxide

Table (4.20) FTIR wavenumber of sample 9 for polystyrene (cork) doping by aluminum oxide

Wave length(cm^{-1})	Symbol and Bond	Function group
520	AL_2O_3	Metallic oxide
700	AL_2O_3	Metallic oxide
1385	N-O	Nitro symmetric
1695	C=O	Carboxylic acid
2900	C-H	Acid
3350	O-H	Water

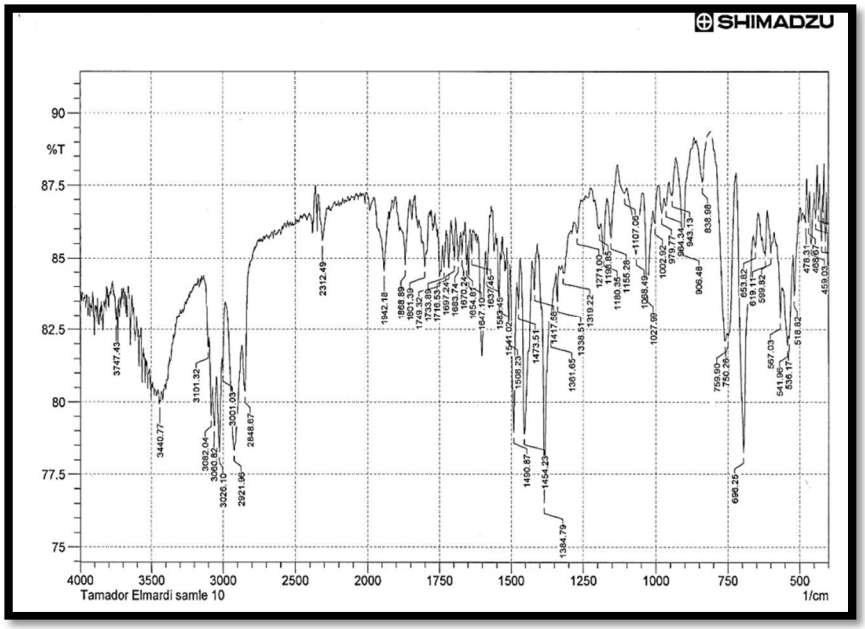

Fig (4.33) FTIR spectrum of sample 10 for polystyrene (cork) doping by aluminum oxide

Table (4.21) FTIR wavenumber of sample 10 for polystyrene (cork) doping by aluminum oxide

Wave length(cm^{-1})	Symbol and Bond	Function group
525	AL_2O_3	Metallic oxide
525	AL_2O_3	Metallic oxide
755	C-H	Ortho distributer aromatic
755	C-H	Ortho distributer aromatic
1375	N-O	Nitro symmetric
1800	C=O	Acid chloride saturate
3000	C-H	Carboxylic acid stretch
3400	O-H	Water

The infrared spectra of synthesized polystyrene(cork) doping by aluminum oxide in different rate of molar (0.1 ,0.2 ,0.3 ,0.4 ,0.5 ,0.6 ,0.7,08 ,0.9 and 0.10) Molarnanoparticles sampleswere recorded by mattson Fourier Transform Infrared Spectrophotometer in the range of 400 to 4000 cm^{-1} which shown from fig(4.24) to fig(4.33). The spectra of all samples have been used to locate the band positions which are given in the Table (4.13) to table (4.21) . In the present study the absorption bands ν1, ν2, ν3, ν4 , ν5,ν6 , ν7,ν8, ν9 ,ν10 and ν11 are found to be around 545 cm^{-1}, 700 cm^{-1}, 750 cm^{-1}, 1025 cm^{-1}, 1450 1cm^{-1} , 1650 cm^{-1} ,1500 cm^{-1} , 2900 cm^{-1}, 3000 cm^{-1} , 3300 $cm^{-1}$and 3450 cm^{-1} respectively for all the compositions. The transmiattance bands within these specific limits reveal the formation of single-phase spinel structure having two sub-lattices tetrahedral (A) site and octahedral (B) site. The (ν1,ν2 and ν3) band around (545 , 700 and 750)cm^{-1} is caused by the metal-oxygen vibration(Al_2O_3) in the tetrahedral sides. This difference in the spectral positions is due to the different values of metal ion-O^{-2} distances for octahedral and tetrahedral sites. The band (ν4) around 1025 $cm^{-1}$is due to C=C stretch bending. The band (ν5 and ν6) around $(1450\ and\ 1650)cm^{-1}$ is associated with the O-H bending vibration .The band (ν7) around 1500 cm^{-1} is due to N=O stretching. (ν8, ν9) around 2900$cm^{-1}$and 3000cm^{-1} is due to the stretching mode of C-H bending .The band (ν10) around 3300 cm^{-1} is due to C≡C stretching. At lastthe band (ν11) around 3450 cm^{-1} is due to O-H stretching vibration of free or absorbed water which implies that the hydroxyl groups are retained in ferrites.

conclusion

This study concluded that the polystyrene (Cork) as an insulating material that can be transformed into a semiconductor by doping it with Aluminum oxide, and since it is considered a cheap industrial and commercial waste and can be obtained easily, it can be a good addition in the field of manufacturing electronic devices such as multijunction in diodes, transistor and integrated circuits as well as the possibility of using it in ultra violet filters.

Recommendations

It is recommended the following recommendations:

1. Conducting the same study taking into account the change in the measurement of the thickness of samples in the Nano-scale boundaries by a fixed amount and noting the extent of this effect
2. Conducting the same study, taking into account the determination of the amount of solvent (benzene) for the cork material, and it shall be fixed for all samples.
3. Study the possibility of deforming the cork with a material other than metal oxides and see if it is possible to obtain a semiconductor from.

References

[1] H. Pereira: Boletim do Instituto dos ProdutosFlorestais – Cortic¸a,1984, 545, 99–112.

[2] C. Fialho, F. Lopes and H. Pereira: For. Ecol. Manage., 2001, 141,251–258.

[3] M. I. d. F. Carrasquinho: Boletim do Instituto dos Produtos Florestais – Cortic¸a, 1987, 583, 17–18.

[4] H. Pereira, M. E. Rosa and M. A. Fortes: IAWA Bull., 1987, 8(3), 213–217.

[5] A. Costa, H. Pereira and A. Oliveira: For. Ecol. Manage., 2003,175, 239–246.

[6] S. K. J. Al- Ani, "*Studies of optical and related properties of thin amorphous films* ", Ph.D. Thesis, Brunel University, (1984).

[7] S. Ben , "Solid State Electronic Devices" , Hall International , Inc. , U.S.A , (1990).

[8] O. Stenz, "*The Physics of Thin Film Optical Spectra*", An Introduction, Winzerlaer Str. 10, 07745 Jena, Germany, (2005).

[9] J. Taunce ,"*Amorphous and Liquid Semiconductors*", Plenum Press, London, (1974).

[10] C.kittel,"Introduction to Solid State Physics",6th .Edition ,Wiley ,(1986) .

[11]B. L. Theraja, "Modern Physics", S. Chandand Company (PVY), New Delhi, (1987).

[12] Ekbal A. M., *"Study of the Physical Properties of ZrO2 :(Co,Ti) Thin Films Prepared by Chemical Spray Pyrolysis*", M.Sc. Thesis, Al-Qadisiya University,(2016)

[13] M.Fox, "*Optical Properties Of Solide*", Oxford University Press Inc, NewYork,(2001).

[14] Sura N. T. , "*Study The Structural, optical and electrical properties of Indium doped Tin oxide thin films deposited by thermal evaporation",* M.Sc. Thesis, kufa University,(2017).

[15] A. Barberis; S. Dettori and M. R. Filiggheddu: J. Arid Environ., 2003, 54, 565–569.

[16] C. Fialho, F. Lopes and H. Pereira: For. Ecol. Manage., 2001, 141, 251–258.

[17] M. I. d. F. Carrasquinho: Boletim do Instituto dos Produtos Florestais – Cortic¸a, 1987, 583, 17–18.

[18] H. Pereira, M. E. Rosa and M. A. Fortes: IAWA Bull., 1987, 8(3), 213–217.

[19] A. Costa, H. Pereira and A. Oliveira: For. Ecol. Manage., 2003, 175, 239–246.

[20] M. Maaˆ taoui, H. Espagnac and N. Michaux-Ferriere: Ann. Bot., 1990, 66, 183–190.

[21] Y. N. Al-Jammal, "*Solid State Physics*", Al-Mousal University Press, Arabic Version, (1990).

[22] B. E. Warren, "*X-RAY diffraction*" Published by Courier Dover, (1990).

[23] L. Gil: 'Cortic¸a: produc¸a˜o, tecnologia e aplicac¸a˜ o'; 1998, Lisbon,
INETI.

[24] B. Groh, C. Hubner and K. J. Lendzian: Planta, 2002, 215, 794–801.

[25] Precision Fourier-New Brault, James W. (1996). "New Approach to formtrans .2896–spectrometer design". Applied Optics. 35 (16): 2891 Bibcode:1996ApOpt..35.2891B doi:10.1364/AO.35.002891. PMID 21085438

[26] Connes, J.; Connes, P, (1966), “Infrared Planetary Spectra by -Near" Fourier Spectroscopy I. Instruments and Results". Journal of the ..(1966) Optical Soc .doi:10.1364/JOSA.56.000896 .910–America. 56 (7): 896

[27] Comparison of the" (Loewenstein, E.V. (1968, Smith, D.R.; Morgan, R.L .434–Infrared Sources". J. Opt. Soc. Am. 58 (3): 433-ance of FarRadi doi:10.1364/JOSA.58.000433

[28] Griffiths, P.; de Hasseth, J. A, (2007), Fourier Transform Infrared, - The Infracord double beam spectrophotometer". Clinical Science. 16 " .2019 0-19404-471-0-Blackwell. ISBN 978-Wiley .(Spectrometry (2nd(2)

Chapter One
Introduction

Chapter Two
Theoretical Background

Chapter Three
Experimental

Chapter Four
Results and Discussion